

CONFIDENTIAL

Copy C 2
RM A54A25

NACA RM A54A25



RESEARCH MEMORANDUM

THE USE OF AREA SUCTION TO INCREASE THE EFFECTIVENESS
OF A TRAILING-EDGE FLAP ON A TRIANGULAR WING OF
ASPECT RATIO 2

By Mark W. Kelly and William H. Tolhurst, Jr.

Ames Aeronautical Laboratory
Moffett Field, Calif.

CLASSIFICATION CANCELLED

Authority *NACA Res. Rep. 10-18-56*

4 RN-108

By *NB 11-2-56* See

CLASSIFIED DOCUMENT

This material contains information affecting the National Defense of the United States within the meaning of the espionage laws, Title 18, U.S.C., Secs. 793 and 794, the transmission or revelation of which in any manner to an unauthorized person is prohibited by law.

NATIONAL ADVISORY COMMITTEE
FOR AERONAUTICS

WASHINGTON

April 1, 1954

APR 1 1954

LANGLEY AERONAUTICAL LABORATORY
LIBRARY, NACA

CONFIDENTIAL



NATIONAL ADVISORY COMMITTEE FOR AERONAUTICS

RESEARCH MEMORANDUM

THE USE OF AREA SUCTION TO INCREASE THE EFFECTIVENESS
OF A TRAILING-EDGE FLAP ON A TRIANGULAR WING OF
ASPECT RATIO 2

By Mark W. Kelly and William H. Tolhurst, Jr.

SUMMARY

A wind-tunnel investigation was conducted to determine the effect of applying area-suction boundary-layer control to a constant-chord plain flap on a triangular wing of aspect ratio 2. Measurements of lift, drag, pitching moment, pressure distribution on the wing and flap, and suction requirements were made for Reynolds numbers from 9.8 to 18.2×10^6 .

The results showed that with small amounts of suction applied near the leading edge of the flap, high lift at relatively low attitudes can be obtained. It was found that the flap effectiveness could be estimated by linear inviscid fluid theory. For the flap deflected 59° and 69° the flap effectiveness was 92 and 85 percent, respectively, of the theoretical value. Some flow separation was observed at each end of the flap. When this separation was partially controlled, the flap effectiveness for both the 59° and 69° deflections was in good agreement with the theoretical value. It was also found that extensive regions of flow separation near the leading edge of the wing had no significant effect on the flap effectiveness as long as the flow reattached to the wing ahead of the 30-percent-chord station.

The suction requirements obtained in this investigation were compared with values estimated from the data of NACA RM A53E06, using the procedure outlined in Appendix A of that report. The comparison indicated that this procedure is probably adequate for use in preliminary design, if a proper choice of reference data is made; that is, suction requirement calculations for area-suction flaps on other triangular wings should be based upon the data of this report, and those for sweptback wings should be based upon the data of NACA RM A53E06.

~~CONFIDENTIAL~~

INTRODUCTION

A major difficulty encountered by aircraft employing low-aspect-ratio triangular wings is the necessity of going to extremely high angles of attack to attain high lift coefficients. Because of this difficulty, it has been necessary to accept both unusually large landing attitudes and rather low values of wing loading for these aircraft to obtain reasonable landing speeds. Trailing-edge flaps have been proposed as a possible means of providing these wings with adequate lift at moderate angles of attack, and a series of tests have been made to establish the characteristics of triangular-wing aircraft equipped with various types of flaps. The results of some of these investigations are presented in references 1, 2, and 3.

Recent tests of a swept wing equipped with a plain flap on which the boundary layer was controlled by suction through a porous area on the flap have shown that large increases in lift can be attained in this manner with only moderate expenditures of power for pumping (ref. 4). Since these large flap lift increments would be particularly useful on low-aspect-ratio triangular wings, it appeared desirable to determine experimentally whether similar lift increments could be obtained from an area-suction flap applied to a wing of this type. In particular, since a large amount of leading-edge flow separation usually is encountered on triangular wings, it was considered important to establish the effect of this separation on the performance of the flap. Further, inasmuch as reference 4 presents methods for estimating the lift increment and power requirements associated with this type of boundary-layer control, it appeared desirable to determine the extent to which these methods could be applied to a wing of substantially different plan form and section.

This report presents the results of tests to determine the effectiveness and power requirements of area-suction boundary-layer control applied to a flap on a triangular wing of aspect ratio 2. Since this investigation was in a large measure parallel to that of reference 4, a special effort has been made in the discussion and analysis to relate these results to those of reference 4.

NOTATION

- b wing span, ft
c wing chord, ft
 \bar{c} mean aerodynamic chord, $\frac{2}{S} \int_0^{b/2} c^2 dy$, ft

- c_n section normal-force coefficient, $\frac{1}{c} \oint P dx$
 C_D drag coefficient, $\frac{\text{external drag}}{q_0 S}$
 C_L lift coefficient, $\frac{\text{lift}}{q_0 S}$
 $C_{L\delta}$ lift coefficient per radian of flap deflection
 C_m pitching-moment coefficient, computed about the quarter-chord point of the mean aerodynamic chord, $\frac{\text{pitching moment}}{q_0 c S}$
 C_Q flow coefficient, $\frac{Q}{U_0 S}$
 C_P power coefficient, $(-P_p)(C_Q)$
 P_0 free-stream static pressure, lb/sq ft
 P_l wing surface static pressure, lb/sq ft
 P_p plenum-chamber static pressure, lb/sq ft
 P wing pressure coefficient, $\frac{P_l - P_0}{q_0}$
 P_p plenum-chamber pressure coefficient, $\frac{P_p - P_0}{q_0}$
 Δp pressure differential across porous material, lb/sq ft
 q_0 free-stream dynamic pressure, lb/sq ft
 Q quantity of air removed through porous surface based on standard density, cu ft/sec
 R Reynolds number, $\frac{U_0 \bar{c}}{\nu}$
 s_r distance along airfoil surface from projected flap hinge line to aft edge of porous opening, in.
 s_f distance along airfoil surface from projected flap hinge line to forward edge of porous opening, in.
 S wing area, sq ft
 S_f flap area, sq ft
 S_R wing area spanned by flap, sq ft

U_0	free-stream velocity, ft/sec
w_0	suction-air velocity, ft/sec
x	distance along airfoil chord, ft
y	spanwise distance from plane of symmetry, ft
Λ_f	sweep angle of flap hinge line, deg
α	angle of attack of wing chord plane, deg
δ_f	flap deflection, deg
ν	kinematic viscosity, ft ² /sec
η	spanwise coordinate, $\frac{2y}{b}$

MODEL AND APPARATUS

A general view of the model installed in the Ames 40- by 80-foot wind tunnel is shown in figure 1. The geometrical characteristics are given in figure 2. Except for the flap, the wing of this model is identical to that used in the investigation of reference 1. The fuselage used in reference 1 was modified by displacing the lower half downward 18 inches to accommodate the boundary-layer-control pumping system, as shown in figure 2.

Suction Flaps

A drawing of the flap is given in figure 3. The flaps rotated about a hinge on the lower surface and could be deflected to either 59° or 69°. The porous material extended rearward 7.90 inches from the reference line for the 59° deflection, and 8.37 inches for the 69° deflection. (The reference line, shown in figure 3(a), is the vertical projection of the flap hinge line on the upper surface of the wing.) The chordwise extent and position of the porous opening for various configurations were controlled by covering portions of the porous material with a nonporous tape approximately 0.003-inch thick.

The porous material used was composed of an electroplated metal mesh sheet backed with white wool felt. The metal mesh sheet was 0.008-inch thick, 11 percent porous, and had 4225 holes per square inch. Two felt backings were used. One was tapered linearly as shown in figure 3(b) and was made from material having the characteristics given in figure 3(c)

for Grade 1 felt. The other had a constant thickness of one-sixteenth inch and had the characteristics given in figure 3(c) for Grade 2 felt.

Pumping System

The boundary-layer-control pumping and ducting systems are shown in figures 3 and 4. Air was drawn from the flap through the wing ducts and plenum chamber into the blower, and then exhausted through the exhaust duct. The spanwise distribution of suction pressure could be controlled with the valves at the entrance to the wing ducts. Since the pressure losses in the wing ducts were insignificant, essentially uniform duct pressure was obtained across the span of the flap with the valves wide open, and they were left in this position during most of the investigation. The flow quantity was obtained by measuring the pressure drop between the plenum chamber and the inlet pipe to the blower. This system was calibrated against standard A.S.M.E. intake orifices. Wing duct pressure measurements were obtained from four static pressure taps located at 24.4, 38.0, 52.0, and 66.0 percent of the wing semispan. The chordwise location of these orifices is shown in figure 3(b). The pump was a modified aircraft engine supercharger driven by two variable-speed electric motors.

TESTS

Initial tests showed that the suction requirements of the boundary-layer control system were not significantly affected by angle of attack. It was also found that, for any particular porous-area configuration and flap deflection, there was a value of suction flow quantity above which significant increases in lift could not be obtained by any reasonable increase in flow quantity. Therefore, it was found convenient to divide the test program into two parts to determine, (1) the suction requirements of the boundary-layer control system, and (2) the longitudinal aerodynamic characteristics of the model with suction applied to the flap.

The data necessary to define the suction requirements of the boundary-layer control system were obtained by varying compressor speed (flow quantity) at a constant angle of attack and free-stream velocity. This was done at uncorrected angles of attack of 0° and 8° for several different chordwise locations and extents of porous area. For some porous-area configurations, these data were also obtained at a few additional angles of attack between 0° and 20° to show any dependence of the suction requirements on angle of attack. Usually, data were taken as the flow quantity was reduced from high values to zero, but checks were made with the flow quantity varied in the opposite direction to detect any hysteresis effects.

After the suction requirements of the boundary-layer control system had been determined, the longitudinal aerodynamic characteristics of the model were obtained. In order to expedite the tests, most of these data were obtained with a constant blower speed sufficient to give a flow coefficient approximately 20 percent above that required to obtain essentially the full flap lift increment.

During the investigation, visual observation of the static pressures on the flap indicated that the flow at the ends of the flap was not as well attached as that near the flap midspan. Therefore, a few devices designed to improve the flow at the ends of the flap were investigated. Some typical results of these tests are included in this report. The effort here was to find devices which would improve the flow, rather than to develop any one device to its ultimate effectiveness.

The investigation covered a range of angles of attack from 0° to 24° , and of Reynolds numbers from 9.8 to 18.2×10^6 . These Reynolds numbers were based upon the mean aerodynamic chord of the model and correspond to a range of free-stream dynamic pressure from 10 to 35 pounds per square foot. Three-component force data, suction flow quantities, and plenum-chamber static pressure were obtained for all configurations tested. In addition, pressure-distribution measurements were usually obtained on the wing and flap, and inside the wing ducts.

RESULTS AND DISCUSSION

Typical Aerodynamic Characteristics

Typical lift, drag, and pitching-moment data are presented in figure 5 for the model with flaps deflected 59° and 69° with¹ and without suction.

Lift.- The data presented in figure 5 show that the use of area suction on the flap resulted in an appreciable increase in lift throughout the angle-of-attack range investigated. (The angle of attack for $C_{l_{max}}$ was beyond the limit of the model pitching mechanism.) The results show that there was a gradual reduction in flap lift increment for angles of attack above 8° due to a spanwise progression of flow separation at the leading edge; a more detailed discussion is presented in the section "Effect of Leading-Edge Separation on Flap Effectiveness." The results reported in reference 4 did not show an appreciable reduction in flap lift increment with angle of attack up to $C_{l_{max}}$. Unlike the wing

¹Unless otherwise specified, data labeled "suction on" were obtained with flow coefficients approximately 20 percent above that required to attach the flow to the flap.

discussed herein, the wing used in that investigation had no significant amount of leading-edge flow separation below $C_{L_{max}}$.

Drag.- The drag data presented in figure 5 show that the effect of applying area suction to the flap was generally to reduce the drag at a given lift coefficient. This result is directly opposite to that reported in reference 4 where the application of area suction to the flap resulted in a definite increase in drag for most lift coefficients. These apparently contradictory results are possible because, in general, the application of suction to the flap may change the total wing drag by (1) changing the profile drag by controlling separation on the flap or by changing the separation pattern elsewhere on the wing, or (2) changing the induced drag by changing the spanwise distribution of flap lift. Since the relative importance of the above factors will vary considerably with wing geometry, it should not be expected that boundary-layer control on the flap will give similar drag results on widely differing wing configurations. For the triangular wing it was found that the extent of flow separation at the leading edge (and, hence, the drag due to this separation) was more a function of angle of attack than it was of wing lift coefficient; thus, at the same lift coefficient, the drag was greater without suction since the higher angle of attack required increased the extent of flow separation at the leading edge. In contrast, the swept wing used in the investigation of reference 4 had, as noted previously, no significant amount of leading-edge separation below the maximum lift coefficient; for that wing the drag increment due to suction is more than accounted for by the change in induced drag.

Pitching moment.- The pitching-moment data presented in figure 5 show that the effect of applying area suction to the flap was primarily to produce a large rearward shift of the center of pressure. There was no significant change in the static stability of the model up to an angle of attack of about 9° , where a forward shift of the aerodynamic center occurred. This forward shift of the aerodynamic center is the result of a loss in lift at the wing tip and a partial loss in effectiveness of the outboard portion of the flap caused by flow separation at the wing leading edge. This change in static stability below $C_{L_{max}}$ was not obtained for the wing used in the investigation of reference 4.

Lift Increment Versus Suction Requirements.

Typical variations of lift coefficient with flow and power coefficients are presented in figure 6. It should be noted that there is a value of flow or power coefficient above which significant increases in lift cannot be obtained by any reasonable increase of power. The coefficients corresponding to this value are designated hereinafter as the critical flow coefficient, $C_{q_{crit}}$, and the critical power coefficient, $C_{p_{crit}}$.

These critical values are determined, as in reference 4, as the value of the flow or power coefficient at which the nearly linear part of the curve begins.

Effect of position of porous area.- Figures 7 and 8 present data showing the effect on $C_{Q_{crit}}$ of changing the location and amount of porous opening. Figure 7(a) shows the effect of varying the location of the forward edge of the porous opening while holding the location of the rearward edge fixed. Figure 7(b) shows the effect of varying the location of the rearward edge of the porous opening while holding the forward edge fixed. Figure 8 presents the effect of varying the location of the porous opening while holding the width of the opening constant. The optimum position of the forward edge of the porous opening was at or slightly ahead of the point of minimum pressure on the flap. No similar easily definable point could be determined for locating the rearward edge of the porous opening. However, it was found that relatively large variations of the location of the rearward edge of the porous opening could be tolerated without severe adverse effects on either C_L or $C_{Q_{crit}}$. All of these results are qualitatively the same as those presented in reference 4 where they are described in more detail.

Effect of free-stream velocity.- The variation of C_L with C_Q and C_p for various free-stream velocities is shown in figure 9. For the range of velocities investigated no effect could be measured. A similar result was also obtained in the investigation of reference 4.

Effect of controlling the chordwise distribution of suction-air velocities.- A limited investigation was made to determine the effects on $C_{Q_{crit}}$ and $C_{p_{crit}}$ of changing the chordwise distribution of suction-air velocity by utilizing tapered felts as discussed in Appendix B of reference 4. The results of this investigation are presented in figure 10(a), and corresponding distributions of suction-air velocity (computed from the pressure drop across the porous material) are shown in figure 10(b). As shown in figure 10(a), the use of tapered felts not only gave the expected reduction in critical flow coefficient but also resulted in a small loss of lift. This loss in lift is believed to be due to general deterioration of the model and a lack of exact duplication of test conditions, rather than to any effect of the tapered felts. Appreciable time had elapsed between the two tests, during which the model had been removed and then replaced in the wind tunnel. No similar loss of lift was noticed in the investigation of reference 4. From figure 10(a) it may be concluded that the use of tapered felts gave approximately a 15-percent reduction in $C_{Q_{crit}}$ but gave no reduction in power coefficient. Examination of the pumping pressures showed that the use of tapered felts resulted in an increased pressure ratio which canceled the power saving from the reduction in flow coefficients. A similar result is discussed in Appendix B of reference 4 in more detail. As in the referenced investigation, the increment of pumping pressure due to duct

losses for this model was insignificant. For an actual aircraft installation where the duct size would be more restricted, the duct losses might not be a negligible proportion of the total pumping head. In this event, the saving in power from a reduction in flow coefficient would be more pronounced, since the power consumed by duct losses is a function of flow quantity to the third power.

Effect of angle of attack on suction requirements.- Figure 11 presents lift coefficient as a function of flow and power coefficients for various angles of attack. The data indicate that for this model there is little change in either $C_{Q_{crit}}$ or $C_{P_{crit}}$ with angle of attack. This is somewhat different from the results presented in reference 4 where an increase in angle of attack, while not significantly affecting $C_{Q_{crit}}$, did give a reduction in pumping pressure so that there was a net reduction in required suction power. The explanation of this difference requires a quantitative knowledge of the change with lift coefficient of the displacement thickness of the boundary layer approaching the flap, and a knowledge of the relationship between this and the pressure distribution over the flap. At the present, it is possible only to infer that the boundary-layer displacement thickness just ahead of the flap on the triangular wing must have been less adversely affected by C_L than was that on the 35° sweptback wing of reference 4.

Comparison of estimated with experimental suction requirements.- Estimates of the suction requirements by the method² outlined in Appendix A of reference 4 have been made for the various configurations tested in this investigation. In view of the large difference in plan form and wing section between the triangular wing and the swept wing of reference 4, it was not expected that these calculations would yield precise predictions of the suction requirements for the triangular wing. However, a comparison of these estimates with experimental data should be useful as an estimate of the maximum error involved in the use of this method. Using

²The method outlined in reference 4 for estimating suction requirements can be stated mathematically as

$$C_Q = C_{Q_1} \frac{(S_R/S) \cos \Lambda_f}{(S_R/S)_1 \cos (\Lambda_f)_1}$$

$$P_p = P_1 \frac{\cos^2 \Lambda_f}{\cos^2 (\Lambda_f)_1} + \frac{\Delta p}{q}$$

where ()₁ refers to the reference data.

data from reference 4 for the model with tapered felts, it was estimated that,³ for the triangular wing, $C_{q_{crit}} = 0.00048$ and $C_{p_{crit}} = 0.0034$.

The experimental suction requirements were $C_{q_{crit}} = 0.00040$ and $C_{p_{crit}} = 0.0037$. This agreement between estimated and experimental suction requirements was perhaps fortuitous and was not this close for the constant-thickness-felt configurations where discrepancies up to the order of magnitude of 50 percent were obtained.

Effect of Leading-Edge Separation on Flap Effectiveness

It was previously stated that at angles of attack above 8° there was some deleterious effect of flow separation at the leading edge on the effectiveness of the suction flap, causing both a reduction in lift-curve slope and in static stability (fig. 5). The pressure-distribution data presented in figure 12 for the wing and flap afford some information as to the causes of these effects. These data indicate that at $\alpha = 0.5^\circ$ the suction flap had induced high lift on the unflapped wing section at 80 percent of the semispan, and that at $\alpha = 8.7^\circ$ this section appeared to have completely separated flow. Also of interest is the fact that at $\alpha = 8.7^\circ$ the flap effectiveness (as estimated by the peak pressures on the flap) at 65 percent of the semispan did not appear to have been affected by a separated-flow region at the leading edge which extended to approximately 20 percent of the chord. In general, it appeared that the suction flap was not significantly affected by leading-edge separation as long as the flow reattached to the wing ahead of the 30-percent wing-chord station. These observations are augmented by the tuft studies of figure 13 and the section c_n vs. α data in figure 14. In figure 14, it is shown that the first loss of lift is on the unflapped portion of the wing with the outboard portion of the flap following shortly after. The midspan of the flap ($2y/b = 0.45$) shows no loss in lift. In fact, the slope of the c_n vs. α curve actually increases at the angles of attack where flow separation and reattachment exist on the forward portion

³Using the data given in figures 24 and 29 of reference 4 in the equations of footnote 2 results in the following estimated requirements for the triangular wing with the suction flap deflected 59° :

$$C_Q = 0.00027 \frac{(0.61)(1.00)}{(0.39)(0.875)} = 0.00048$$

$$P_p = (-5.3) \left(\frac{1.00}{0.765} \right) + (-0.2) = -7.1$$

$$C_p = (C_Q)(-P_p) = (0.00048)(7.1) = 0.0034$$

of the chord. Consideration of the above factors would appear to indicate that the loss in lift and static stability obtained from this model might be prevented, or at least delayed to higher angles of attack, by the use of a constant-percent-chord flap instead of a constant-chord flap, since this would lead to less induced loading near the wing tip.

Flap-End Effects

The pressure-distribution data presented in figure 12 indicated that the flow near the ends of the flap was not as successfully controlled by area suction as that near the flap midspan. This observation was also supported by tuft studies such as those presented in figure 13. Various area-suction-configuration changes were made to improve the flow at the ends of the flap, such as increasing the chordwise extent of area suction and changing the spanwise distribution of suction velocity so as to remove more boundary-layer air from these regions, but no significant improvement was obtained.

Effect of fences at flap tip.- The tuft studies presented in figure 13 show a decided inflow of air from the tip of the wing spilling down onto the tip of the flap. In an attempt to restrict this side flow onto the flap, a series of fences located at the flap tip were investigated. Data from some of these investigations are presented in figures 15, 16, and 17. It will be noted that the lift curve in figure 15 for the model with a full-chord fence has a pronounced jog between angles of attack of 6.6° and 8.7° . This jog was caused by a thick wake from an area of leading-edge separation inboard of the fence flowing down along the fence and onto the flap. When the upper surface fence was cut back to begin at 40 percent of the chord, the jog in the lift curve was eliminated. The pressure-distribution data presented in figure 16 for 0° angle of attack show that the fence improved the flow at both the 65-percent- and 80-percent-semispan stations. In addition, the fence altered the stalling characteristics of these two wing sections appreciably as shown by the section data of figure 17. While the fence did provide large changes in section normal-force coefficient, the over-all effect on the wing was small, since only a small portion of the wing area was involved.

Separation at flap root.- Relatively severe flow separation was encountered on the inboard end of the flap, as indicated by the pressure distributions for the 25-percent-semispan station in figure 12 and the tuft studies of figure 13. The cause of this separation was indicated by tuft studies and boundary-layer total-head measurements to be due to the inability of the fuselage boundary layer to negotiate the severe adverse pressure gradient caused by the flap. The resulting separation produced a rather large wake which spread over a sizable portion of the flap. An attempt to restrict the area covered by this wake was made by

placing a trailing-edge fence on the flap at about twice the boundary-layer thickness from the fuselage. However, the boundary layer on the outboard side of the fence apparently separated so that the amount of flow separation on the flap was increased. Figure 18 presents data for the model equipped with two turning vanes placed on the fuselage so as to direct the fuselage boundary layer downward, parallel to the upper surface of the flap. These data show that the turning vanes did provide a significant improvement in flap lift, especially for the model with the flap deflected 69° where this separation at the root was severe. The pressure distributions presented in figure 19 for the 25-percent-span station indicate somewhat improved flow over the flap but not complete attachment. Visual observation of tufts showed no improvement in the flow pattern. Apparently further improvements in lift are possible here if sufficiently powerful control of the fuselage boundary layer can be obtained.

Further investigation was made of the model with a gap 1.5 times the fuselage boundary-layer thickness cut between the end of the flap and the fuselage. Data for this configuration are presented in figure 20, where it is seen that the lift at 0° angle of attack was not changed, although the flap area had been reduced by approximately 6 percent by the gap cutout.

Comparison of Theoretical and Experimental Flap Lift.

Figure 21 presents a comparison of the lift at 0° angle of attack obtained experimentally from this investigation with the linear inviscid fluid theory of reference 5.⁴ It is seen that, while the effectiveness of the unmodified suction flap was below the theoretical estimates, the improvement of the flow at the ends of the flap resulted in close agreement with theory. It should be mentioned that past experience with flaps on this triangular wing (fig. 10 of ref. 3) indicates that experimental lift can exceed the values estimated by the method of reference 5 by about 20 percent. (The cause of this discrepancy has been suggested in references 3 and 5 to be due to using the two-dimensional $d\alpha/d\delta$ concept below

⁴The theoretical flap effectiveness was calculated from

$$C_{L\delta} = \int_0^1 \frac{d\alpha}{d\delta} \frac{dC_{L\delta}}{d\eta} d\eta$$

(eq. (9), ref. 5) by dividing the flap into seven spanwise strips and performing the integration numerically. The values of $d\alpha/d\delta$ used were taken from the "theoretical" curve on figure 3, reference 5, using streamwise flap-to-wing-chord ratios.

the aspect ratios for which it accurately applies.) It would therefore be inferred that the experimental lift values given here could be increased by further refinements to the area-suction flap. Whether or not this is actually the case depends essentially on how nearly the Kutta condition was experimentally satisfied across the flap span, and in the absence of quantitative experimental information about this, the question of precisely how much more lift can be attained by flap refinements cannot be answered here.

Comparison With Other Flaps Tested on Triangular Wings

The increment in lift at 0° angle of attack obtained from the area-suction flap of this investigation is compared in figure 22 with that obtained from more conventional-type flaps on triangular wings of nearly equal aspect ratio. Since the flaps being compared are of widely different sizes, it is necessary to adjust the lift coefficients of each flap by dividing by the ratio of flap to wing area, S_f/S . (For the double-slotted flap, the flap area used was that of the main flap only.) Figure 22 indicates that the single- and double-slotted flaps compare well with the area-suction flap at equal flap deflections. However, they do not operate as effectively at the highest flap deflection as does the suction flap.

CONCLUDING REMARKS

The results of a wind-tunnel investigation of an aspect ratio 2 triangular wing equipped with area-suction flaps indicated that high lift at relatively low attitudes can be obtained from this configuration with low suction requirements. These results were generally similar to those previously obtained from an investigation of a 35° sweptback wing with suction flaps (ref. 4).

For the triangular wing at 0° angle of attack with suction flaps deflected 59° , a flap lift increment of 0.64 was attained for a flow coefficient of 0.00053. With the flaps deflected 69° the corresponding lift increment was 0.69 for a flow coefficient of 0.00090. It was observed that there was an area of partially separated flow at each end of the flap, particularly at the flap root where, apparently, the fuselage boundary layer was caused to separate and transversely contaminate the flow on the flap. These end effects were more severe for the flap deflected 69° than they were for the 59° deflection. Partial control of these end losses resulted in flap lift increments of 0.71 and 0.79 for the flap deflected 59° and 69° , respectively. These values were in good agreement with theoretical flap lift increments estimated by inviscid fluid theory. In view of this agreement it is believed that the lift

increments of area-suction flaps on other wings can be estimated by the theory of reference 5 with sufficient accuracy for most design purposes.

It was found that extensive regions of separation could exist on the wing ahead of the flap without any significant adverse effects on the flap lift. This appeared to be so as long as the flow reattached to the wing ahead of the 30-percent-chord station.

Estimates of the suction requirements for the flap were made by the procedure outlined in reference 4. Comparison of these estimates with results of the various configurations tested in this investigation showed discrepancies up to 50 percent. In view of the extreme differences in plan form and wing section between the models these discrepancies are not surprising. In general, it is believed that if suction-requirement calculations for similar triangular wings are based on the data from this investigation, and those for swept wings are based on the data of reference 4, the procedure will give results satisfactory for use in preliminary design.

Ames Aeronautical Laboratory
National Advisory Committee for Aeronautics
Moffett Field, Calif., Jan. 25, 1954

REFERENCES

1. Graham, David, and Koenig, David G.: Tests in the Ames 40- by 80-Foot Wind Tunnel of an Airplane Configuration With an Aspect Ratio 2 Triangular Wing and an All-Movable Horizontal Tail - Longitudinal Characteristics. NACA RM A51B21, 1951.
2. Riebe, John M., and MacLeod, Richard G.: Low-Speed Wind-Tunnel Investigation of a Thin 60° Delta Wing With Double Slotted, Single Slotted, Plain, and Split Flaps. NACA RM L52J29, 1949.
3. Graham, David: The Low-Speed Lift and Drag Characteristics of a Series of Airplane Models Having Triangular or Modified Triangular Wings. NACA RM A53D14, 1953
4. Cook, Woodrow L., Holzhauser, Curt A., and Kelly, Mark W.: The Use of Area Suction for the Purpose of Improving Trailing-Edge Flap Effectiveness on a 35° Sweptback Wing. NACA RM A53E06, 1953
5. DeYoung, John: Theoretical Symmetric Span Loading Due to Flap Deflection for Wings of Arbitrary Plan Form at Subsonic Speeds. NACA Rep. 1071, 1952. (Supersedes NACA TN 2278.)

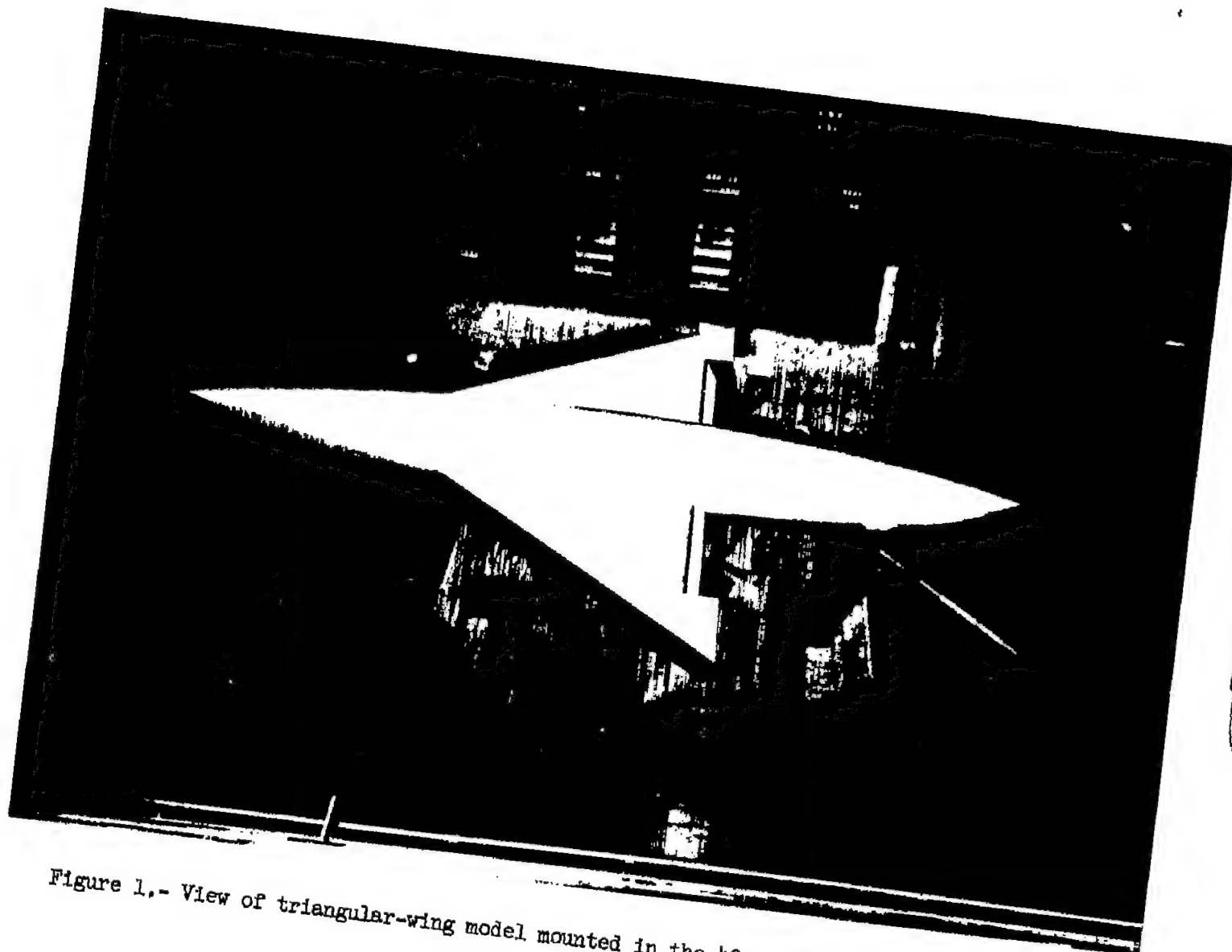


Figure 1.- View of triangular-wing model mounted in the 40- by 80-foot wind tunnel.

A-18077

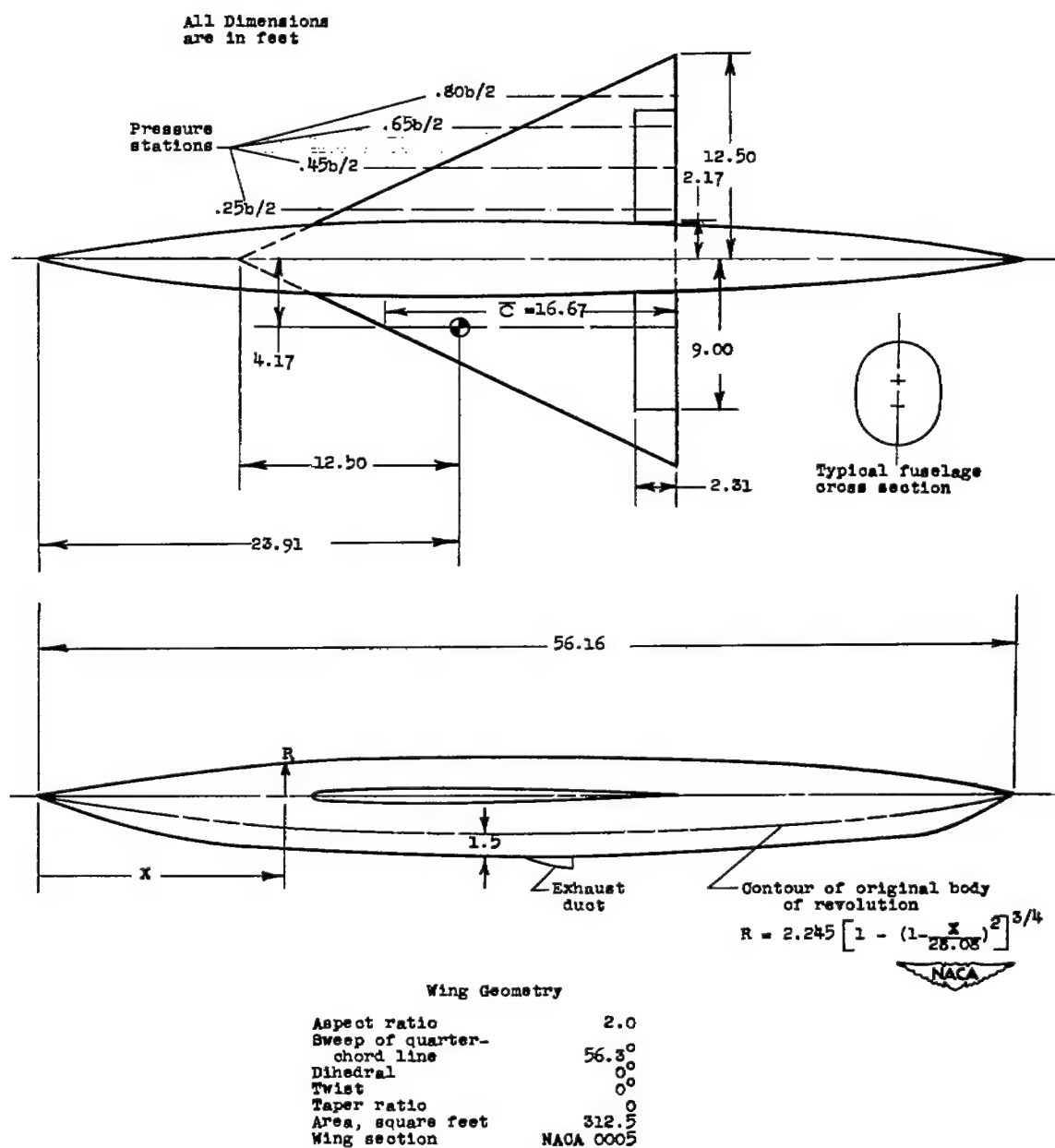
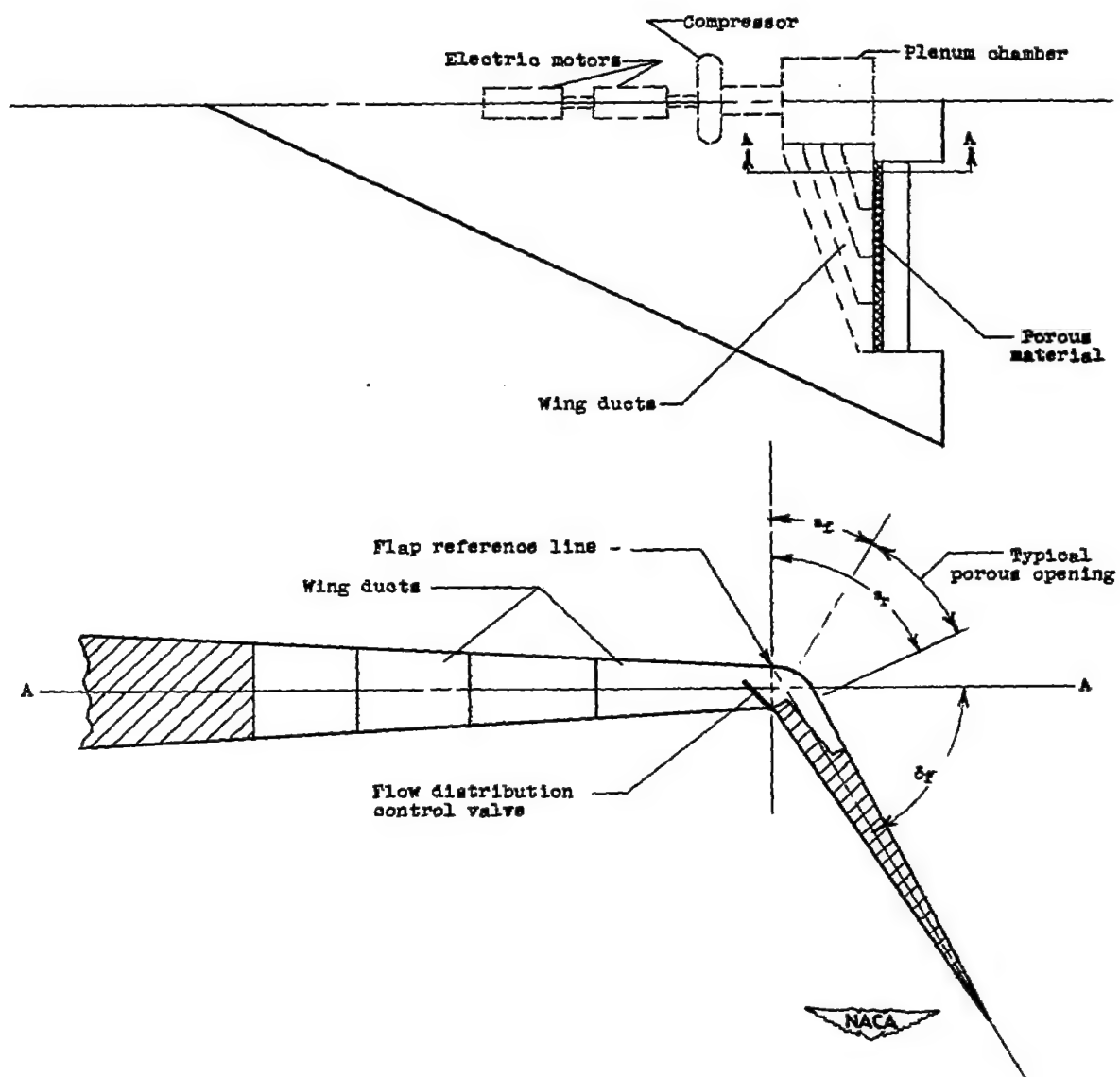


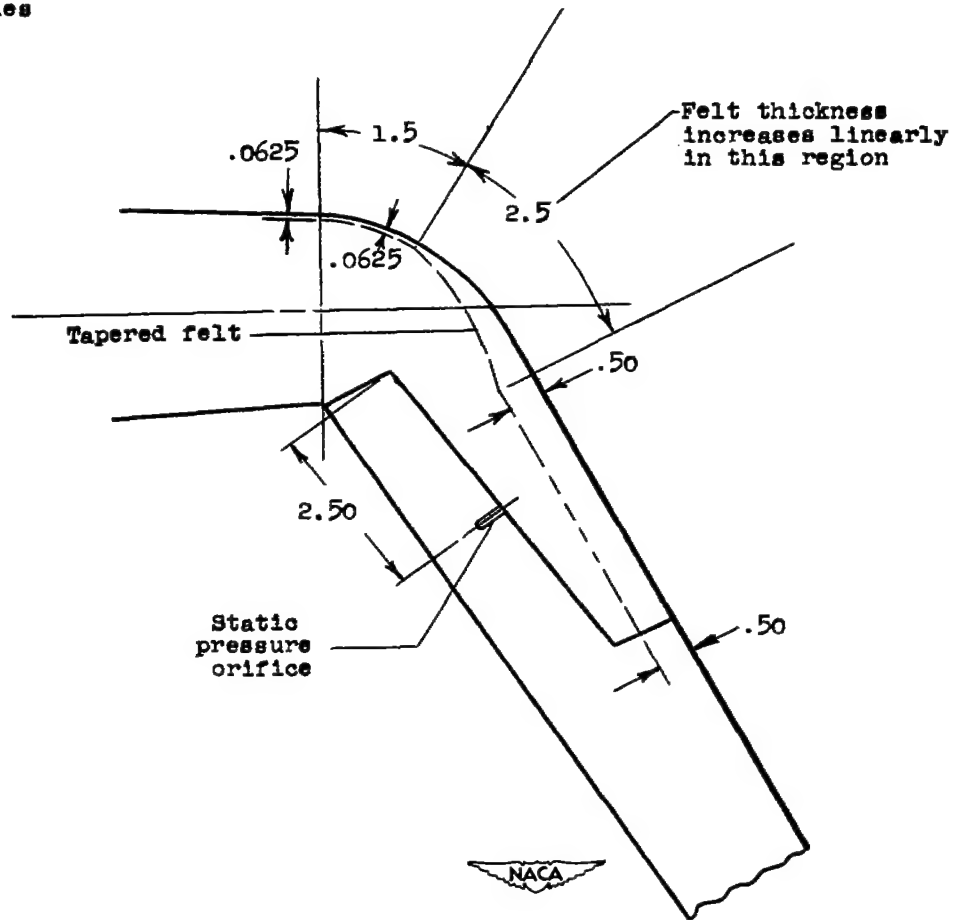
Figure 2.- Geometric characteristics of the model.



(a) General arrangement.

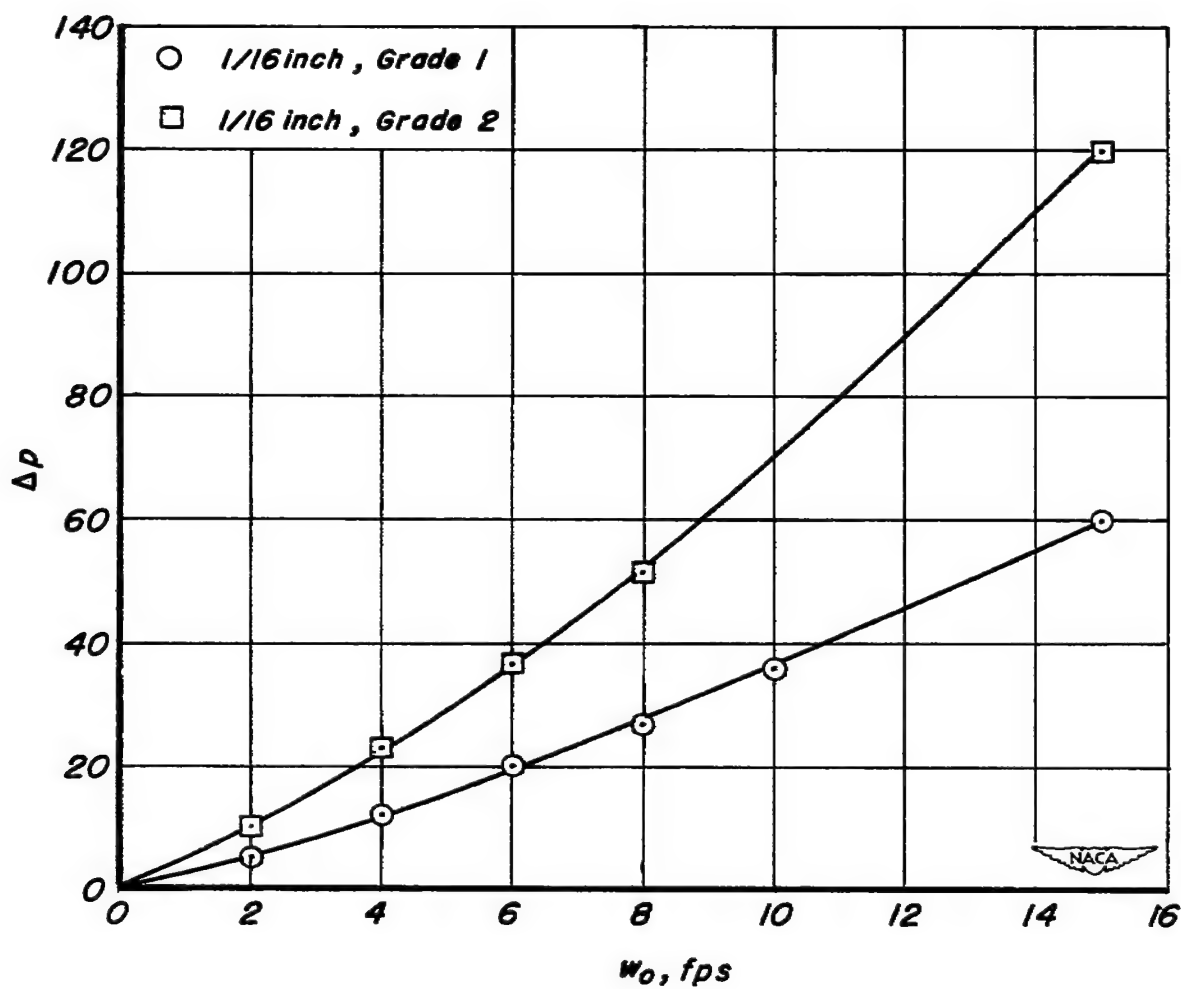
Figure 3.- Boundary-layer control system.

All dimensions
are in inches



(b) Flap details.

Figure 3.- Continued.



(c) Flow characteristics of felt backing.

Figure 3.- Concluded.

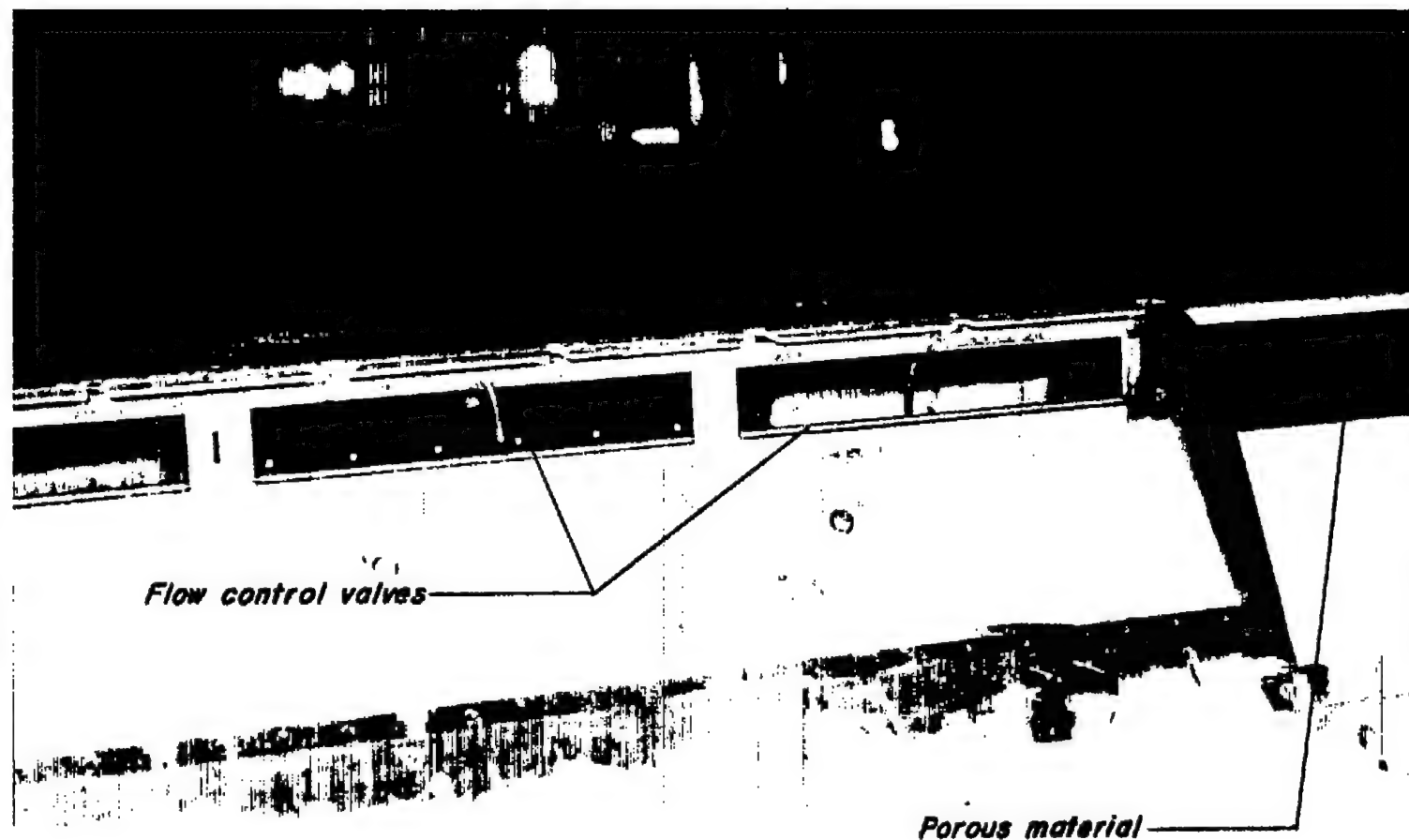


Figure 4.- Photograph of porous material insert and wing ducts.

A-18347.1

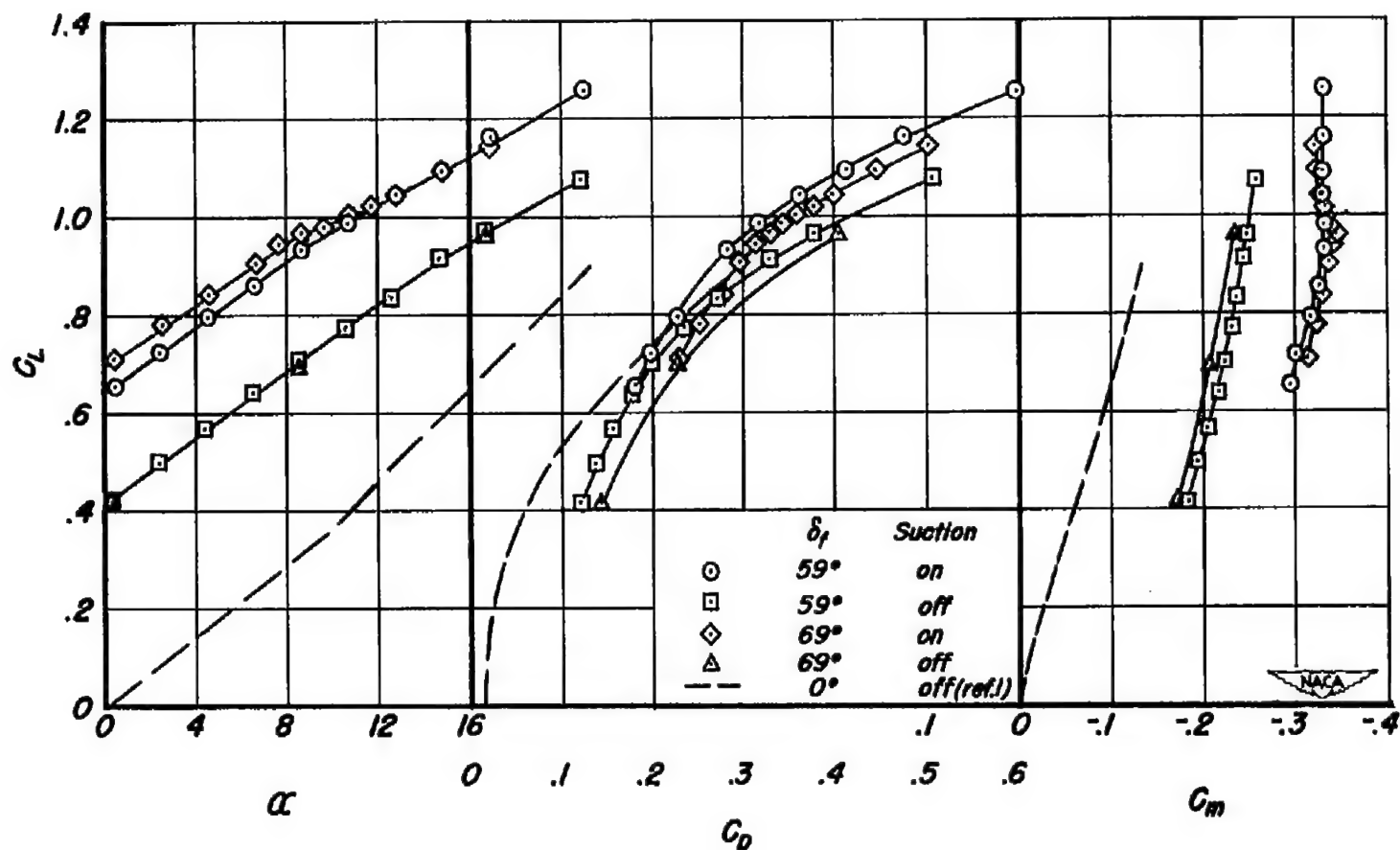


Figure 5.- Aerodynamic characteristics of the model with the suction flap deflected 59° and 69° with and without suction.

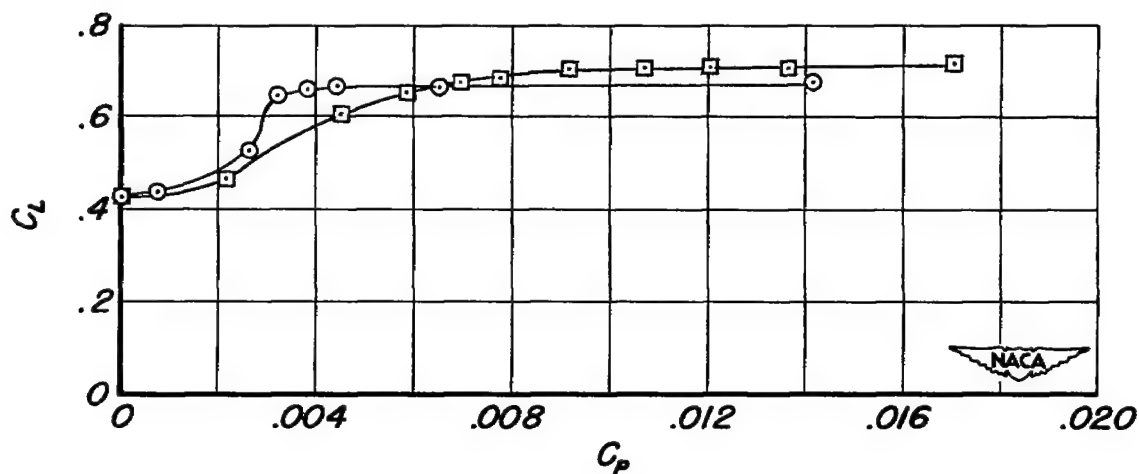
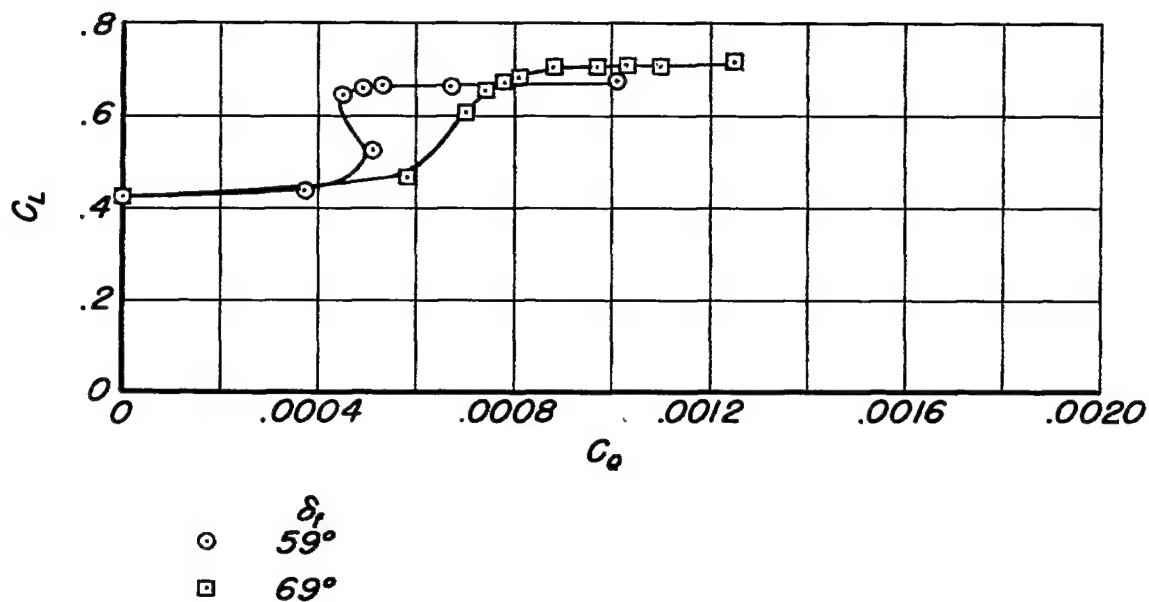
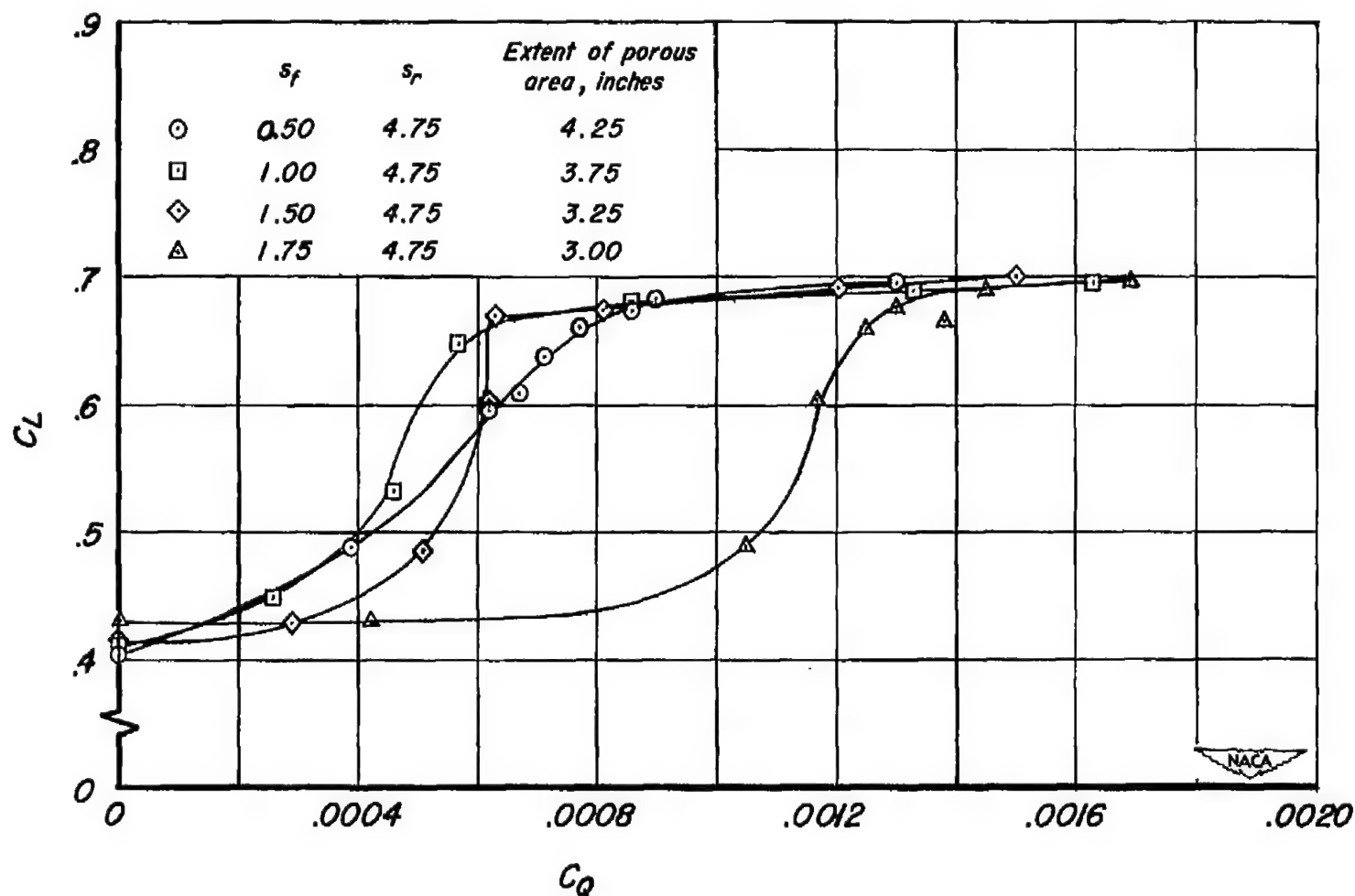
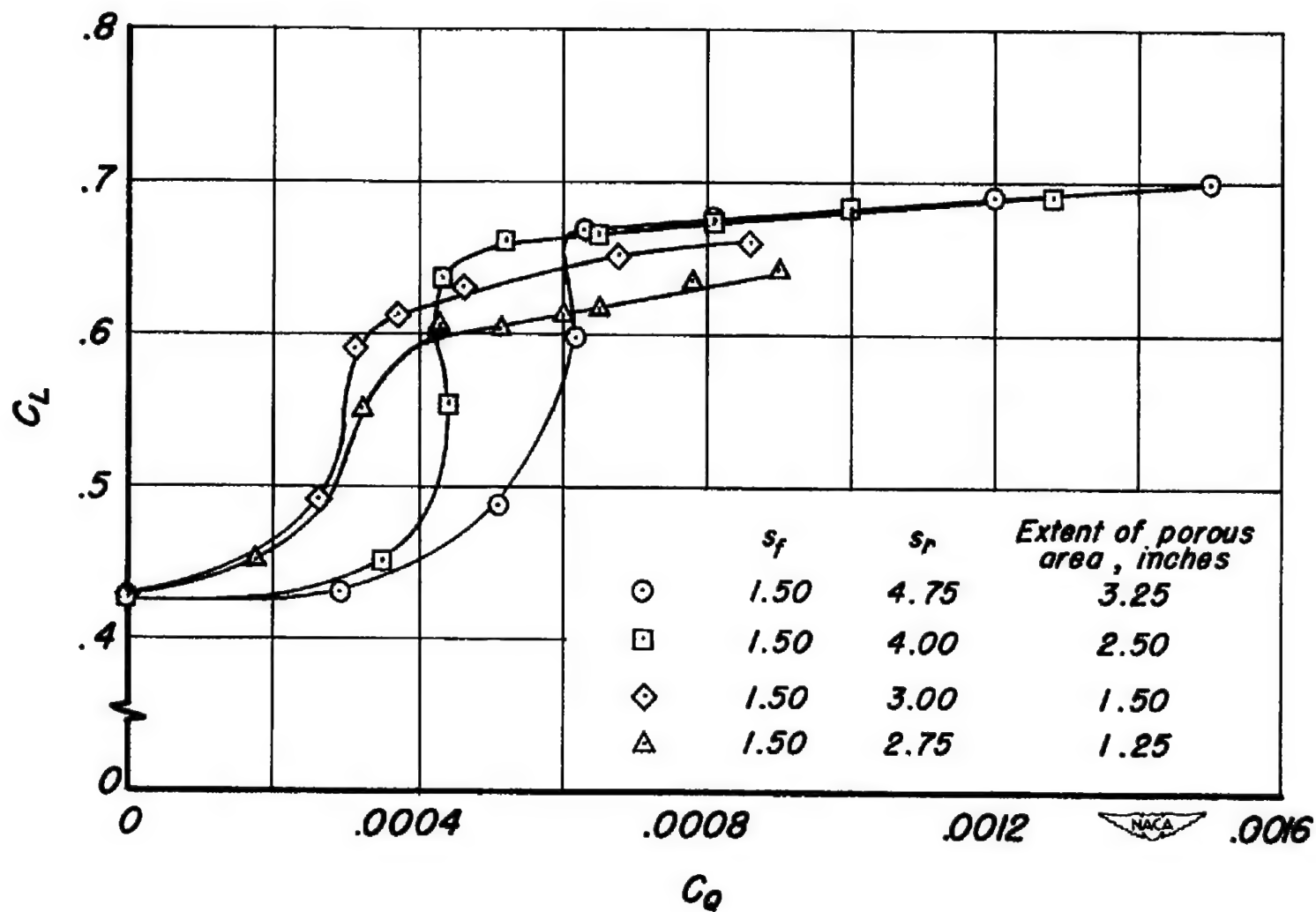


Figure 6.- Typical variation of flap lift increment with flow and power coefficient for two flap deflections; $\alpha = 0.5^\circ$.



(a) Effect of varying location of forward edge of porous area (location of rearward edge fixed).

Figure 7.- Variation of flap lift increment with flow coefficient for various positions and extents of porous area; $\delta f = 59^\circ$, $\alpha = 0.5^\circ$.



(b) Effect of varying location of rearward edge of porous area (location of forward edge fixed).

Figure 7.- Concluded.

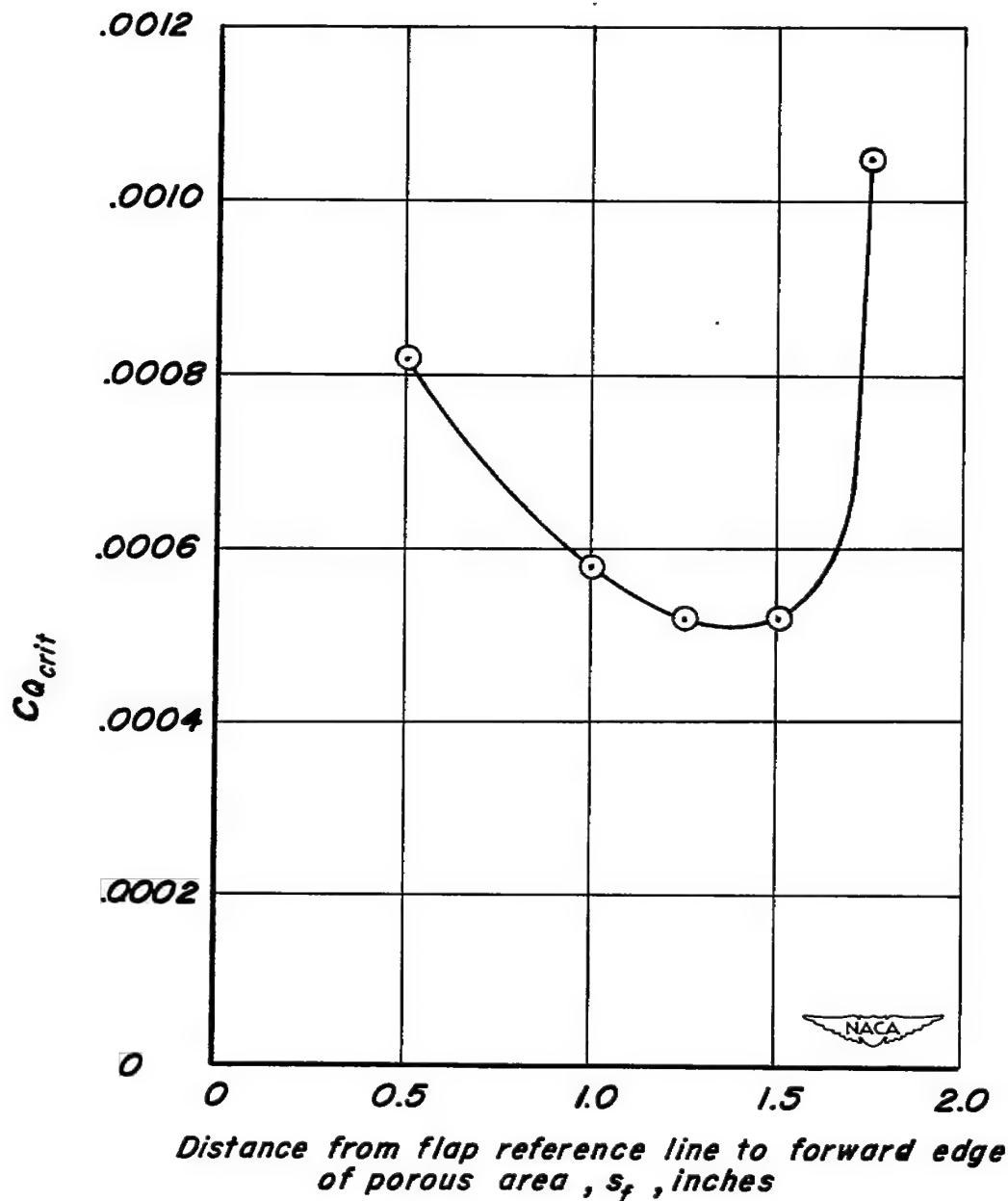


Figure 8.- Variation of critical flow coefficient with position of porous area for a constant chordwise extent of porous area of 2.50 inches; $\alpha = 0.5^\circ$, $\delta_f = 59^\circ$.

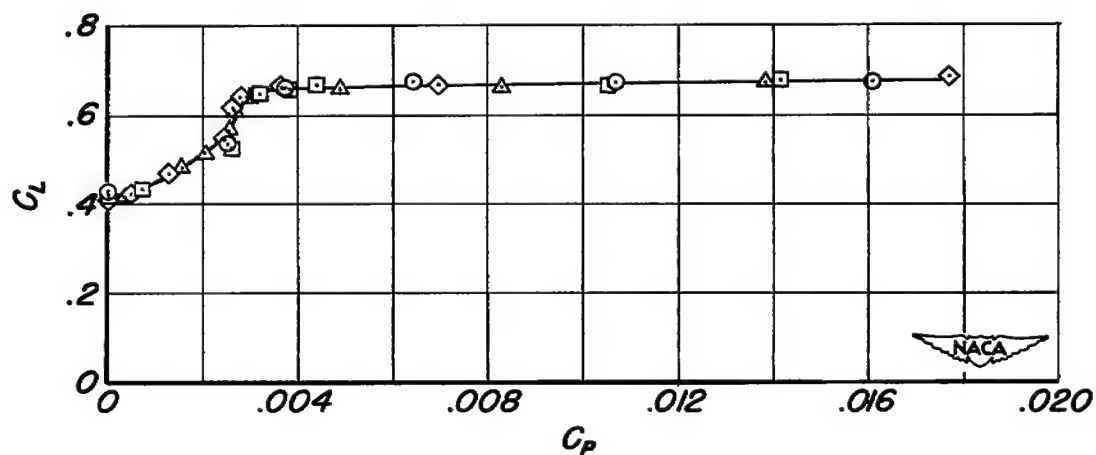
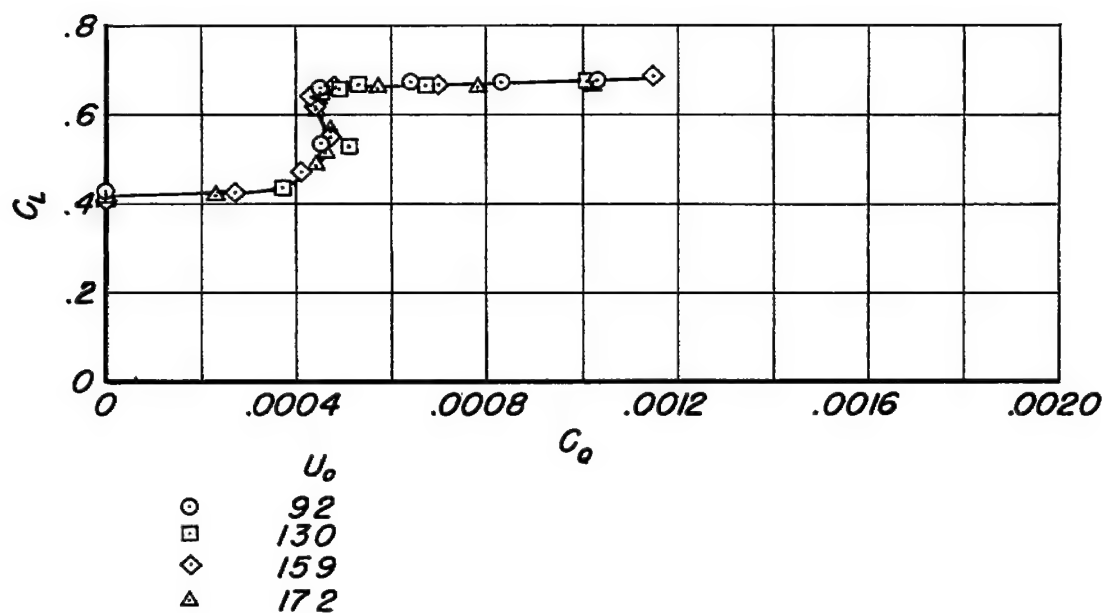
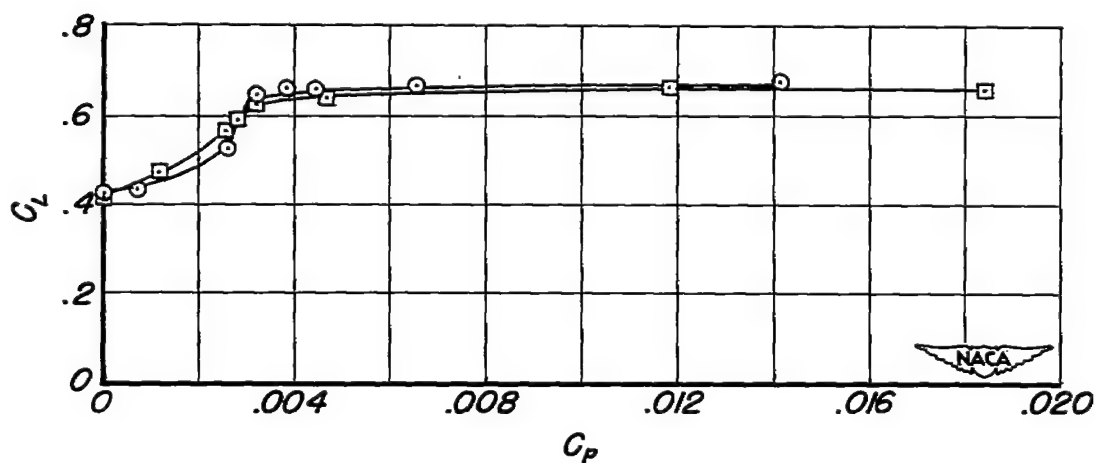
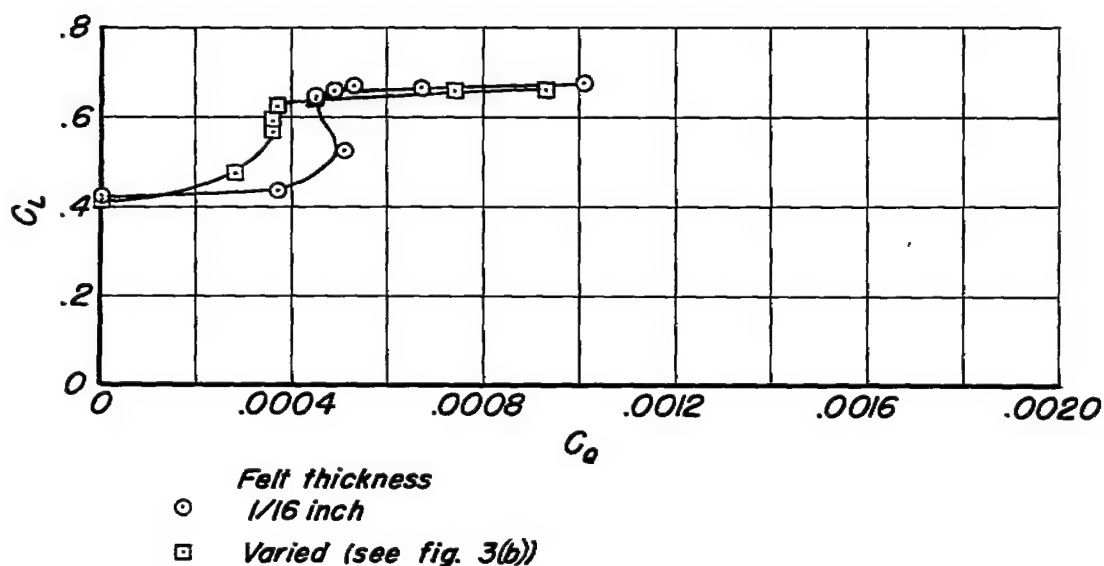
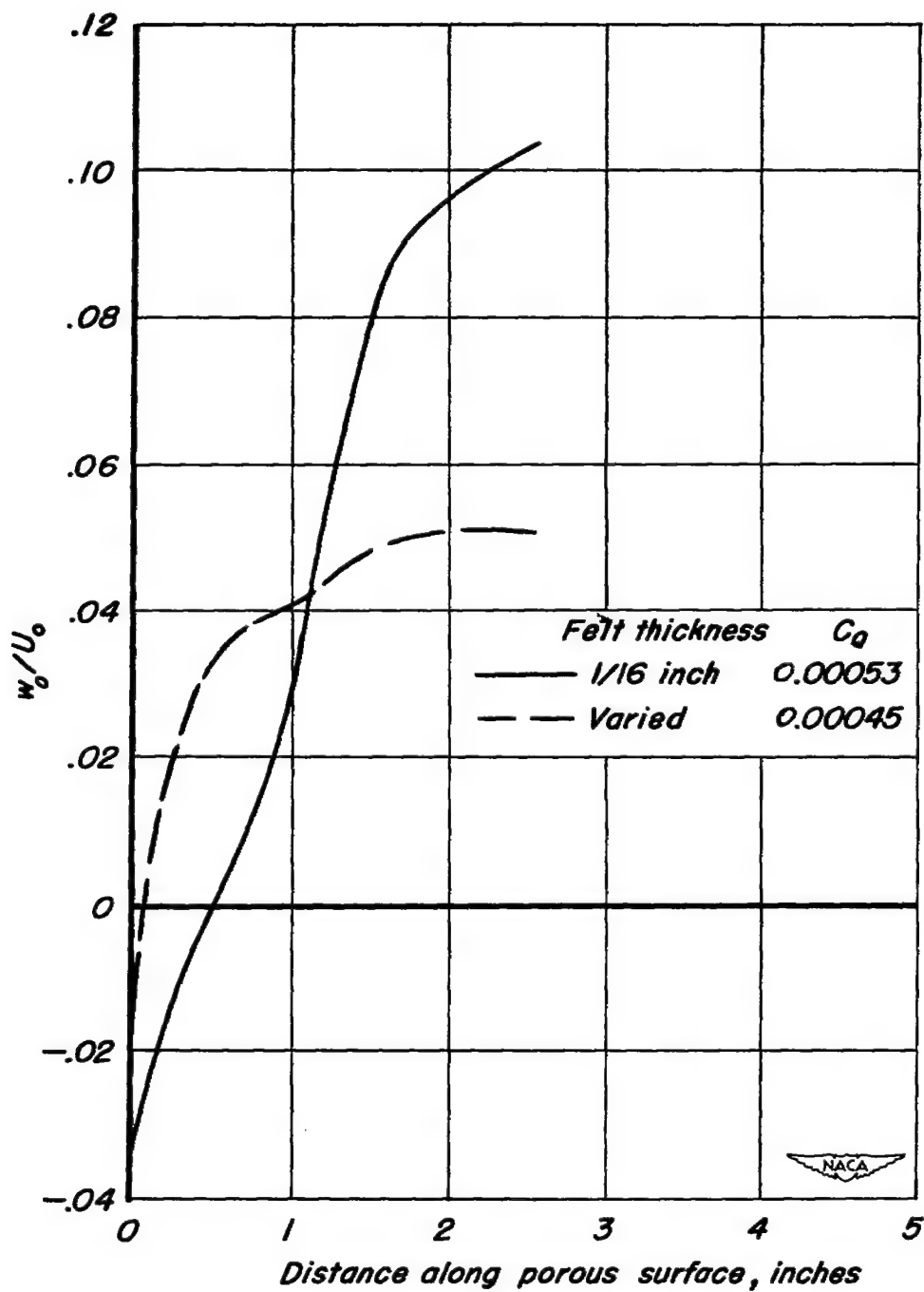


Figure 9.- Variation of lift coefficient with flow and power coefficient for various free-stream velocities; $\alpha = 0.5^\circ$, $\delta_f = 59^\circ$, $S_f = 1.50$ in., extent of porous area = 2.50 in.



(a) Variation of lift coefficient with flow and power coefficient.

Figure 10.- The effects of controlling the chordwise distribution of suction-air velocities; $\delta_f = 59^\circ$, $\alpha = 0.5^\circ$, $S_f = 1.50$ in., extent of porous area = 2.50 in.



(b) Chordwise distribution of suction-air velocities.

Figure 10.- Concluded.

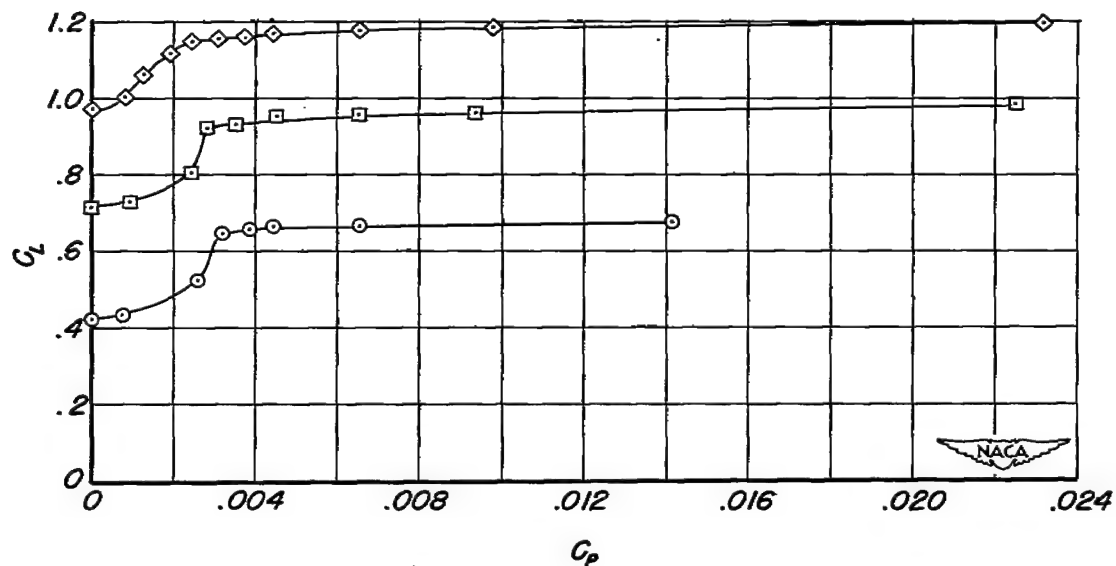
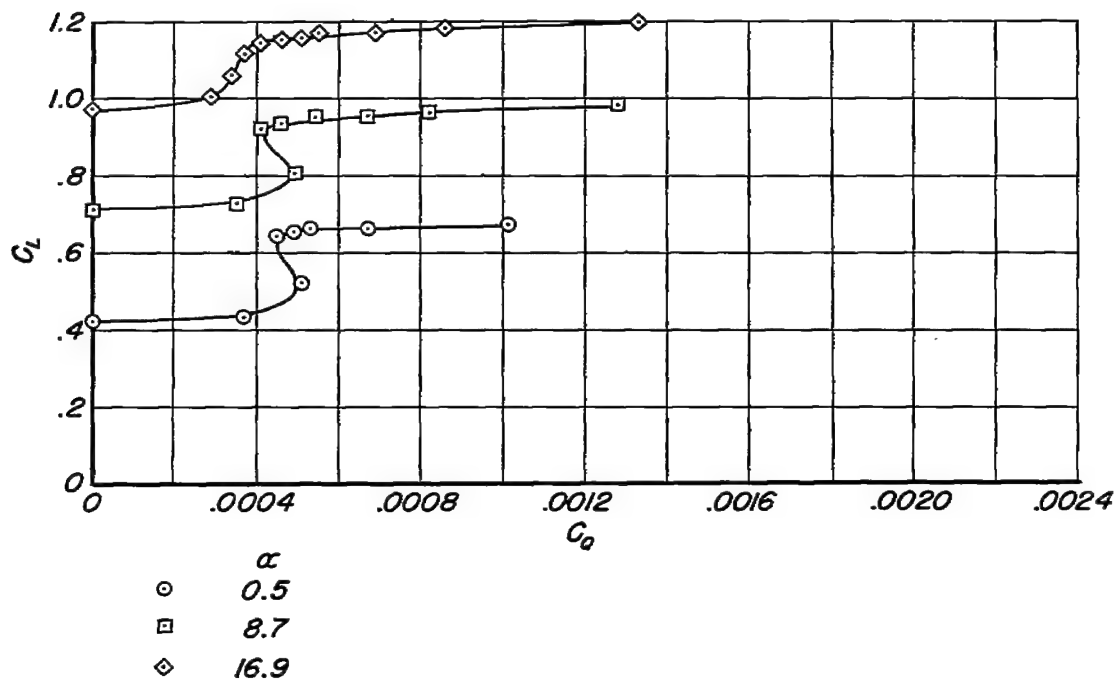


Figure 11.- Typical variation of lift coefficient with flow and power coefficients for various angles of attack; $\delta_f = 59^\circ$.

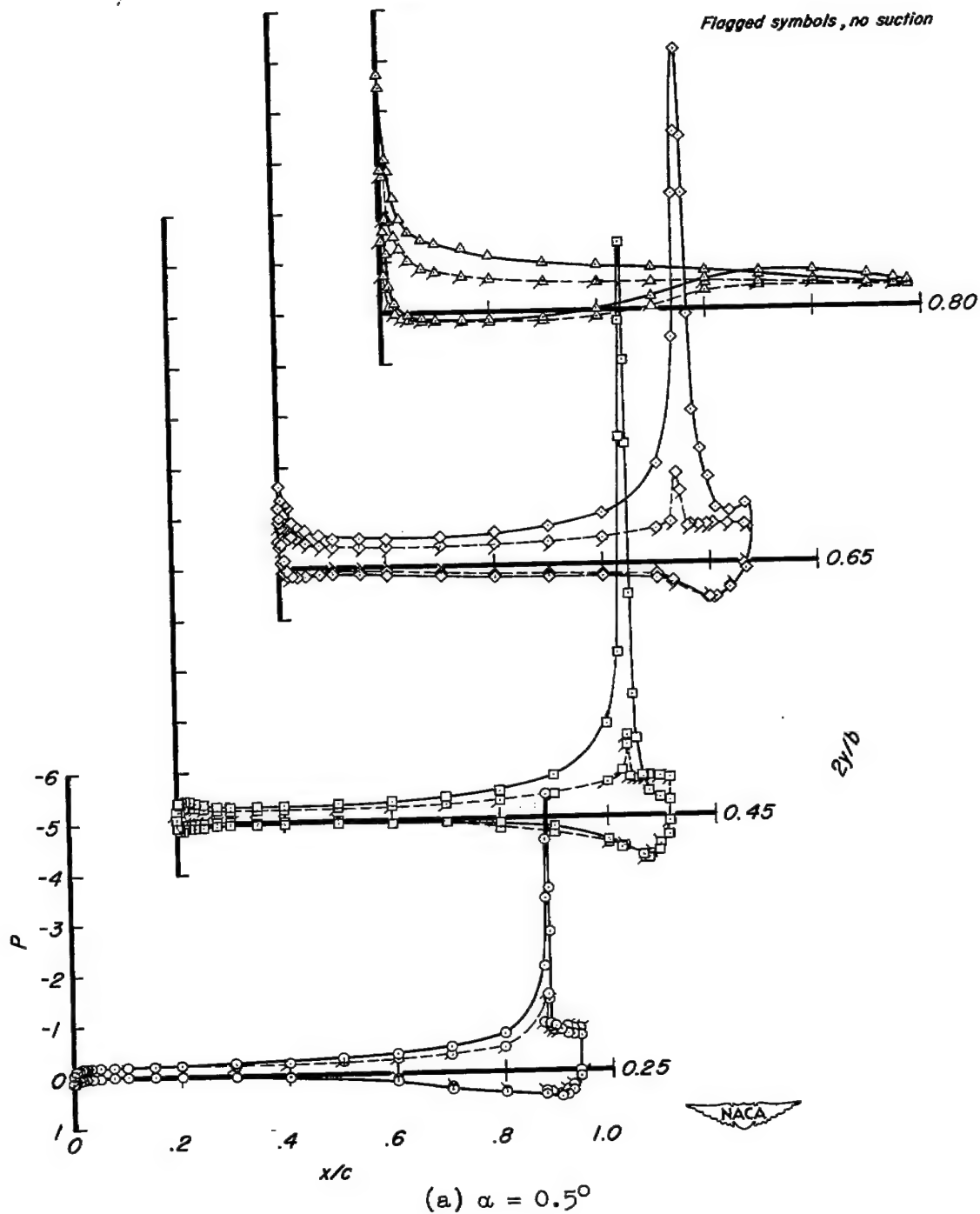
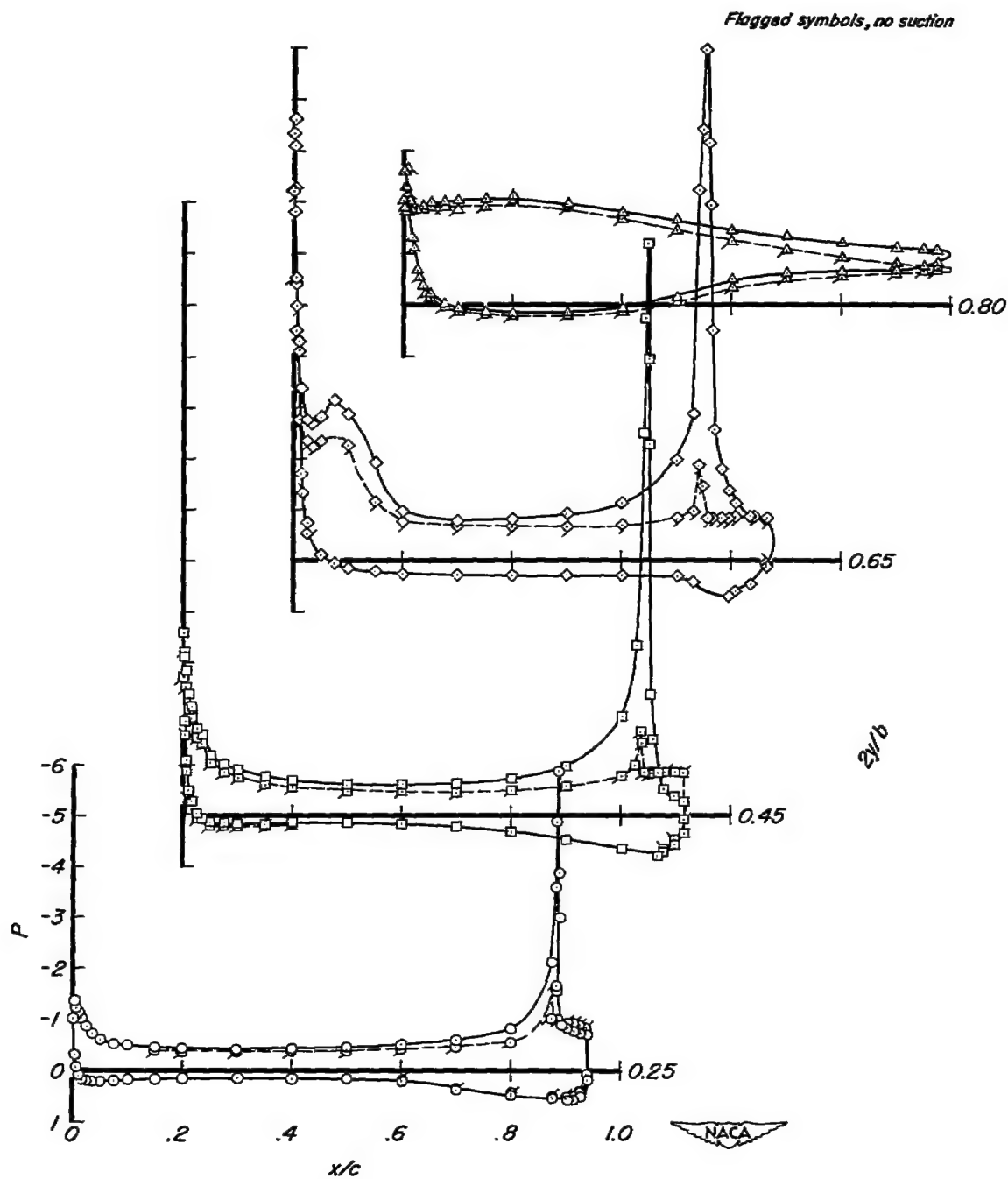
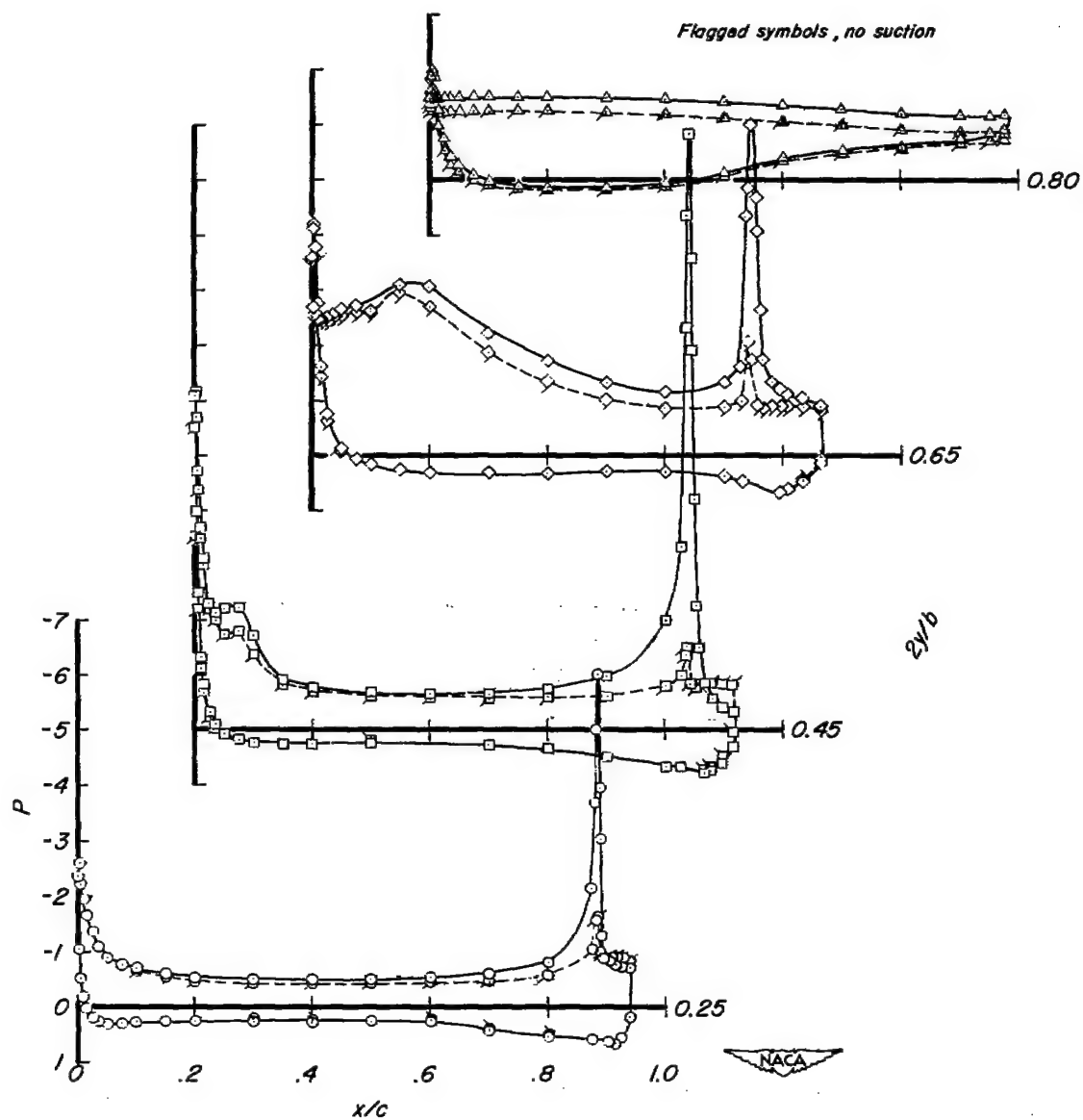


Figure 12.- Chordwise pressure distributions for the model with and without suction; $\delta_f = 59^\circ$.



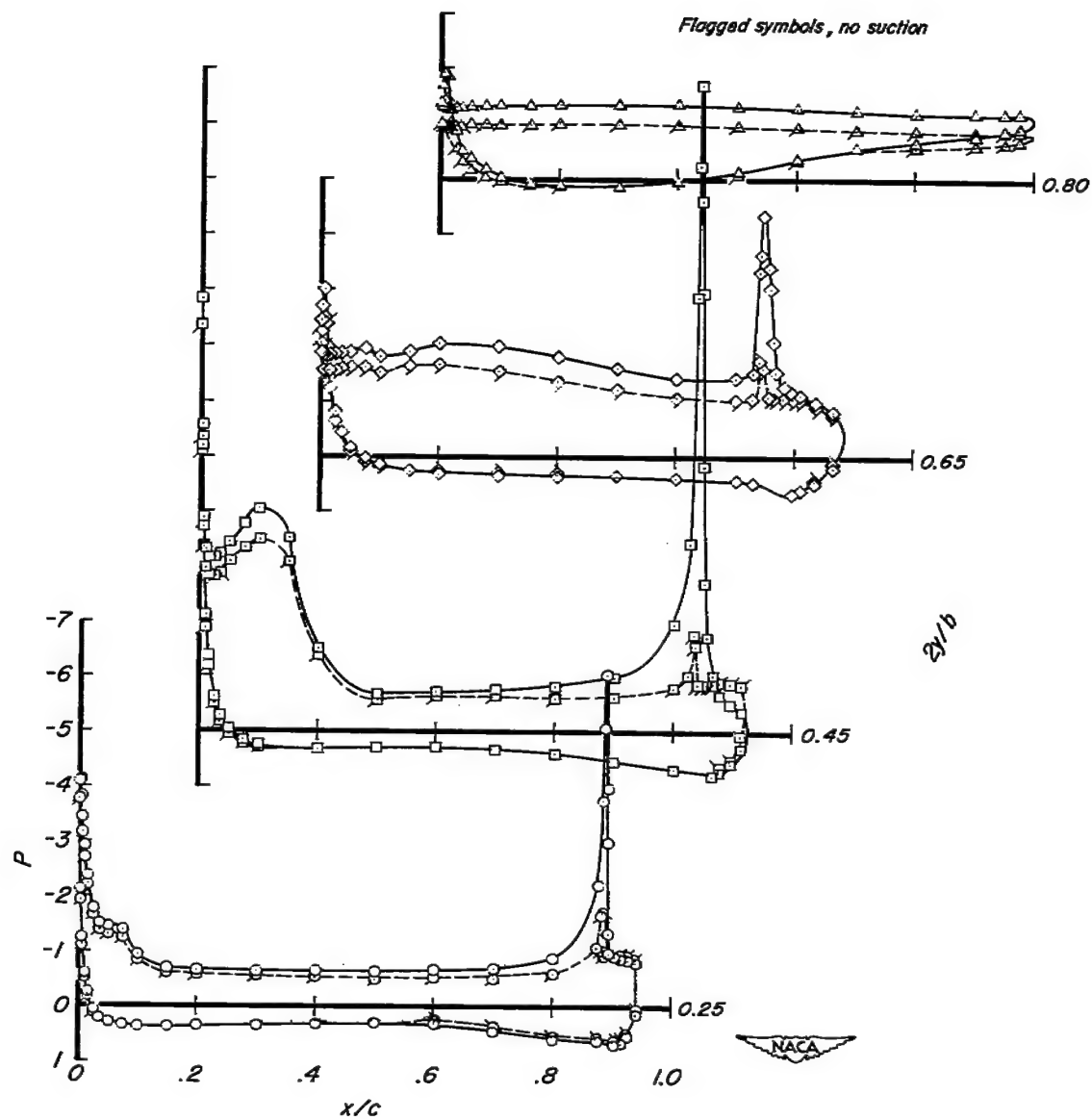
(b) $\alpha = 8.7^\circ$

Figure 12.- Continued.



(c) $\alpha = 12.8^\circ$

Figure 12.- Continued.



(d) $\alpha = 16.9^\circ$

Figure 12.- Concluded.

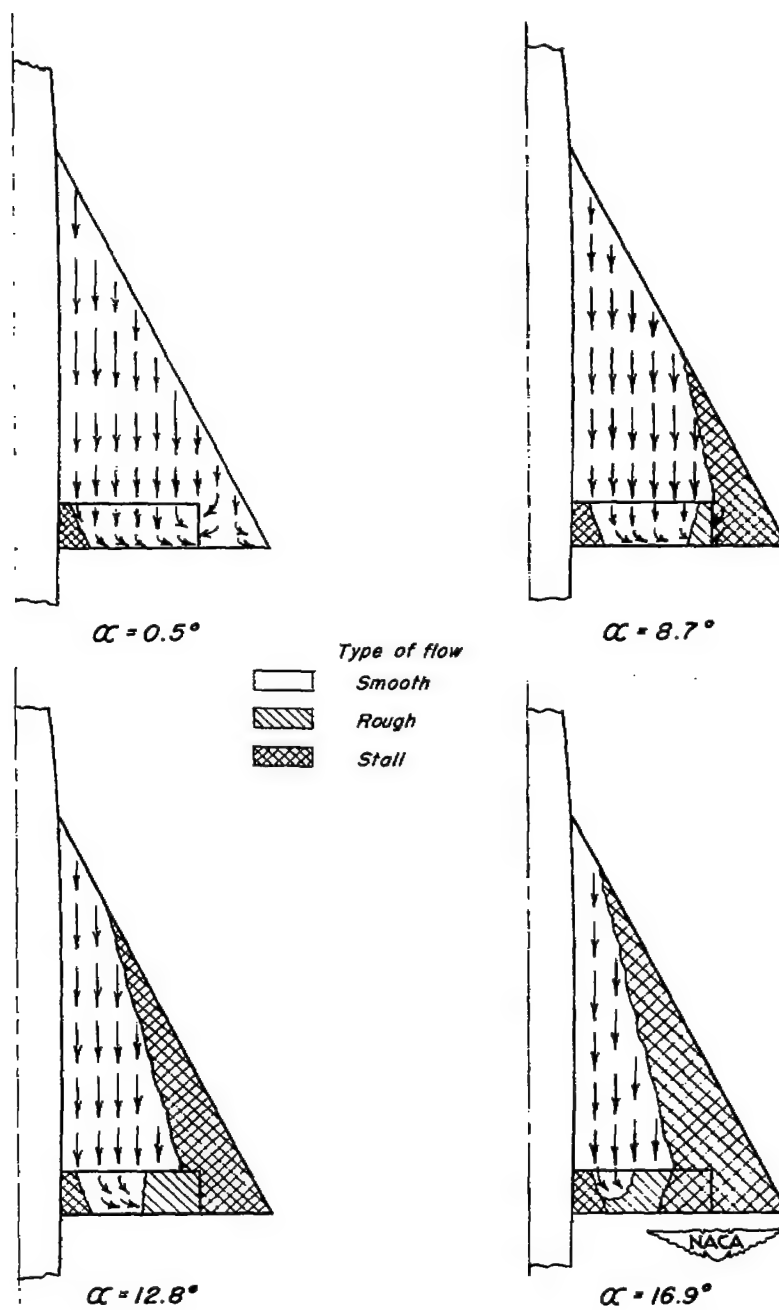
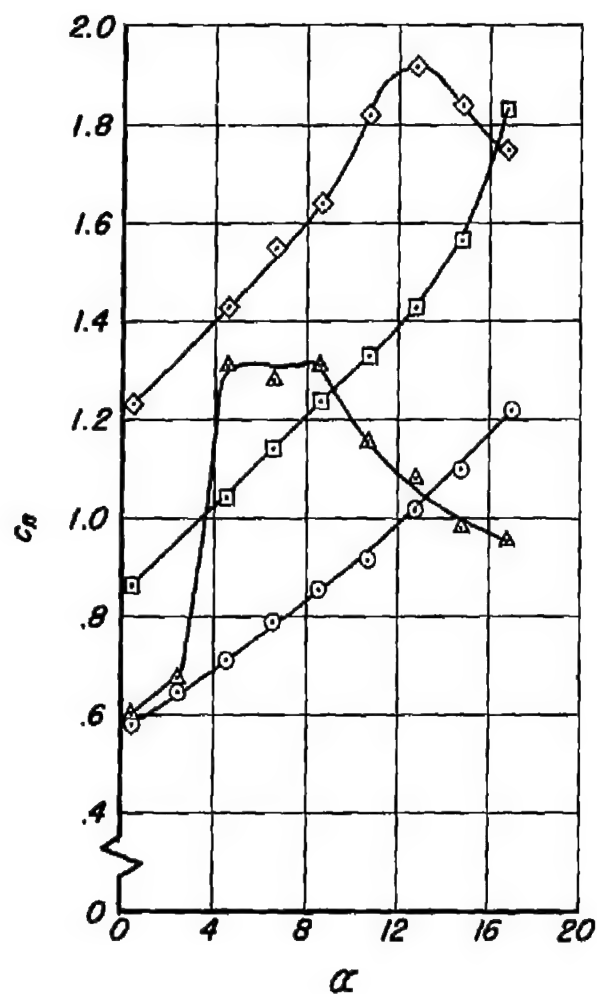
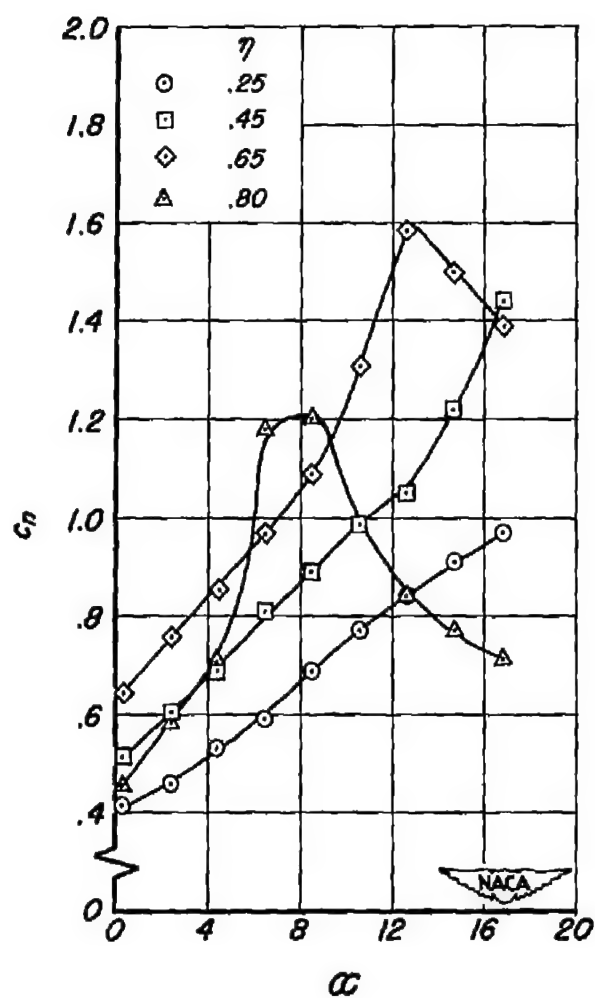


Figure 13.- Progression of flow separation with angle of attack for the model with suction; $\delta_f = 59^\circ$.

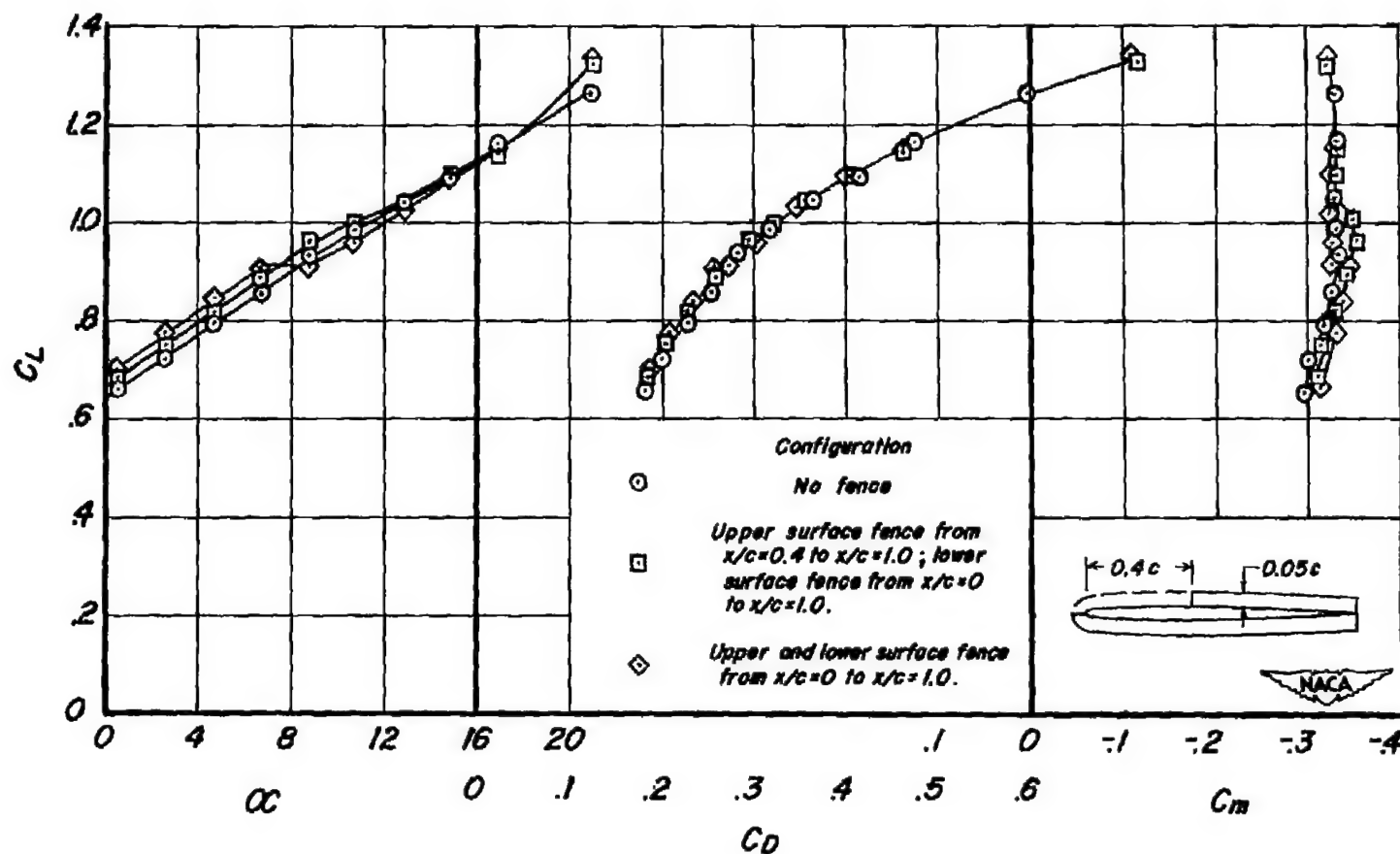


(a) Suction on.



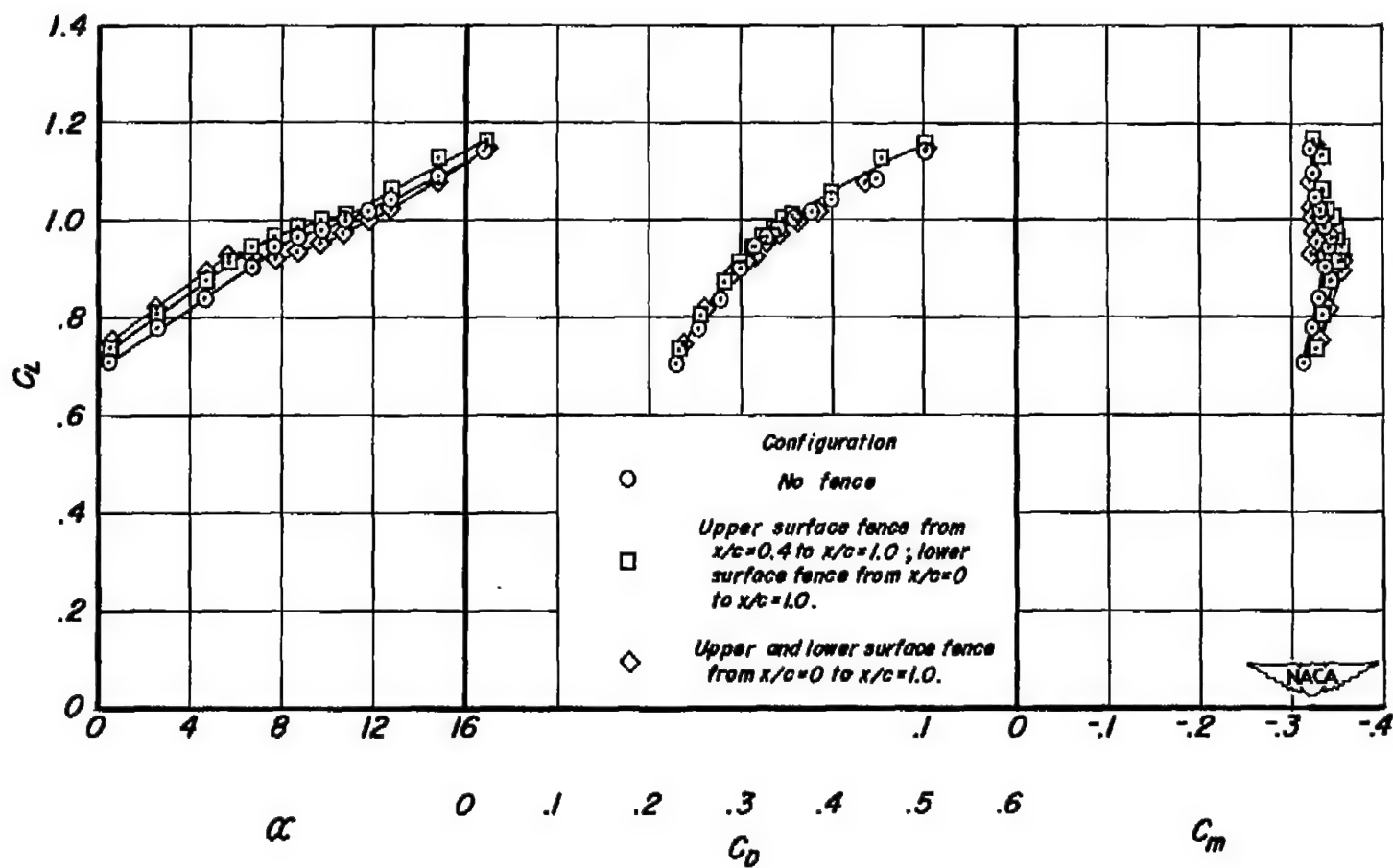
(b) Suction off.

Figure 14.- Variation of section normal-force coefficient with angle of attack; $\delta_f = 59^\circ$.



(a) $\delta_f = 59^\circ$

Figure 15.- Aerodynamic characteristics of the model with the suction flap deflected and with a fence installed at the flap tip.



(b) $\delta_F = 69^\circ$

Figure 15.- Concluded.

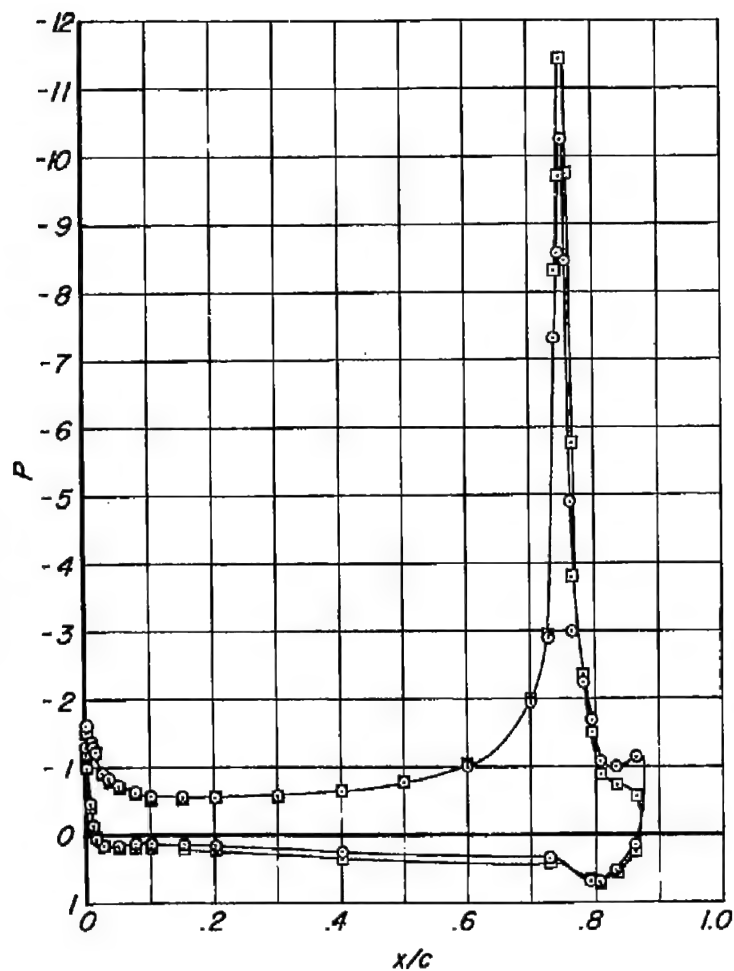
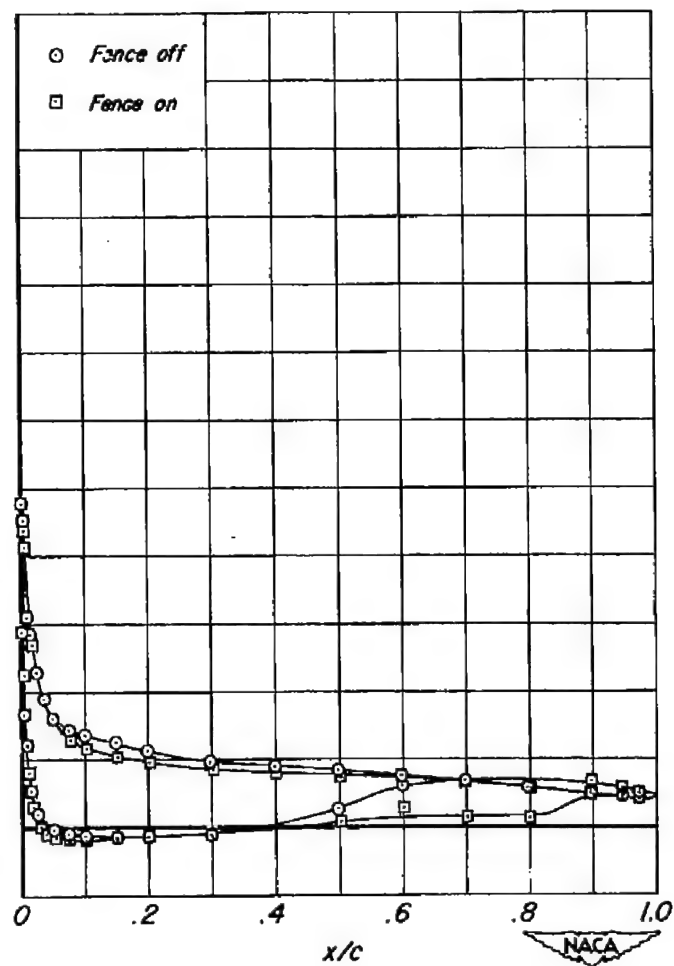
(a) $\eta = 0.65$ (b) $\eta = 0.80$

Figure 16.- Typical chordwise pressure distributions for the model with and without fence; suction on, $\delta_F = 59^\circ$, $\alpha = 0.5^\circ$.

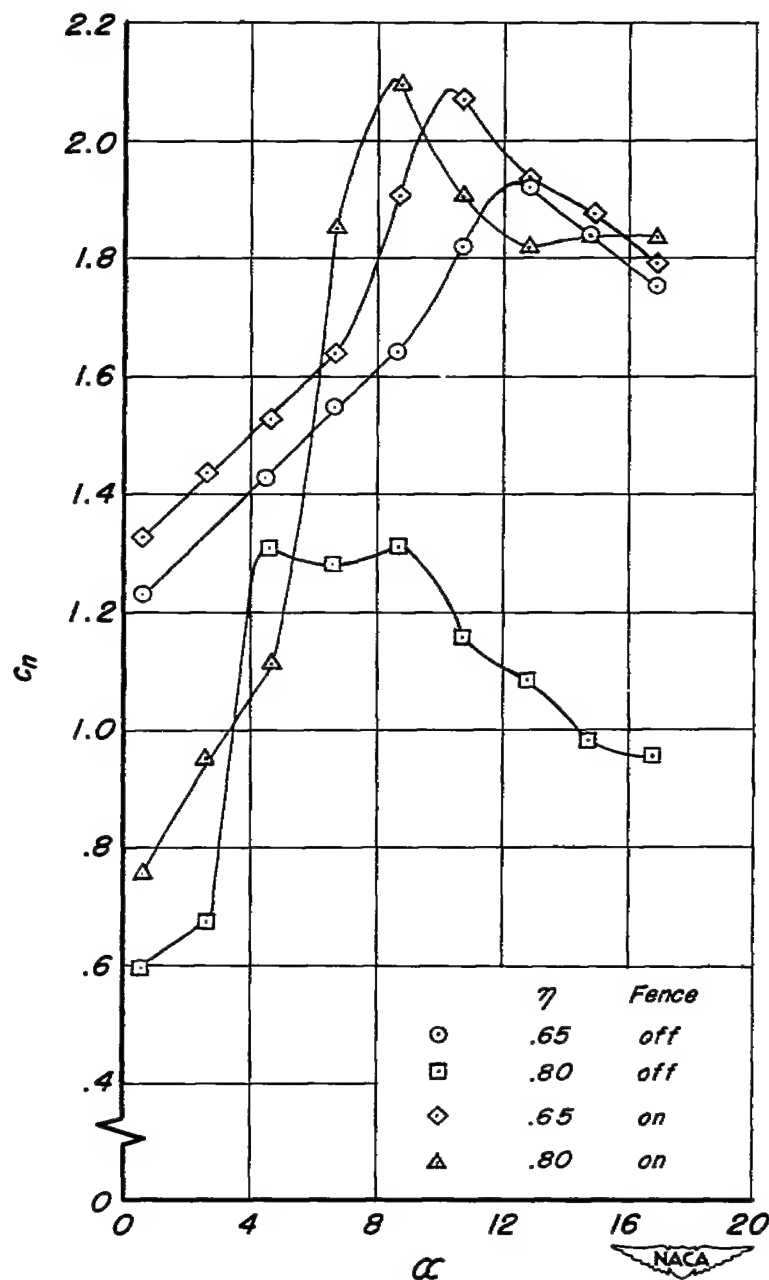


Figure 17.- Variation of section normal-force coefficients with angle of attack with and without a fence at the flap tip; suction on, $\delta_f = 59^\circ$, full-chord lower-surface fence, upper-surface fence from $0.40c$ to $1.00c$.

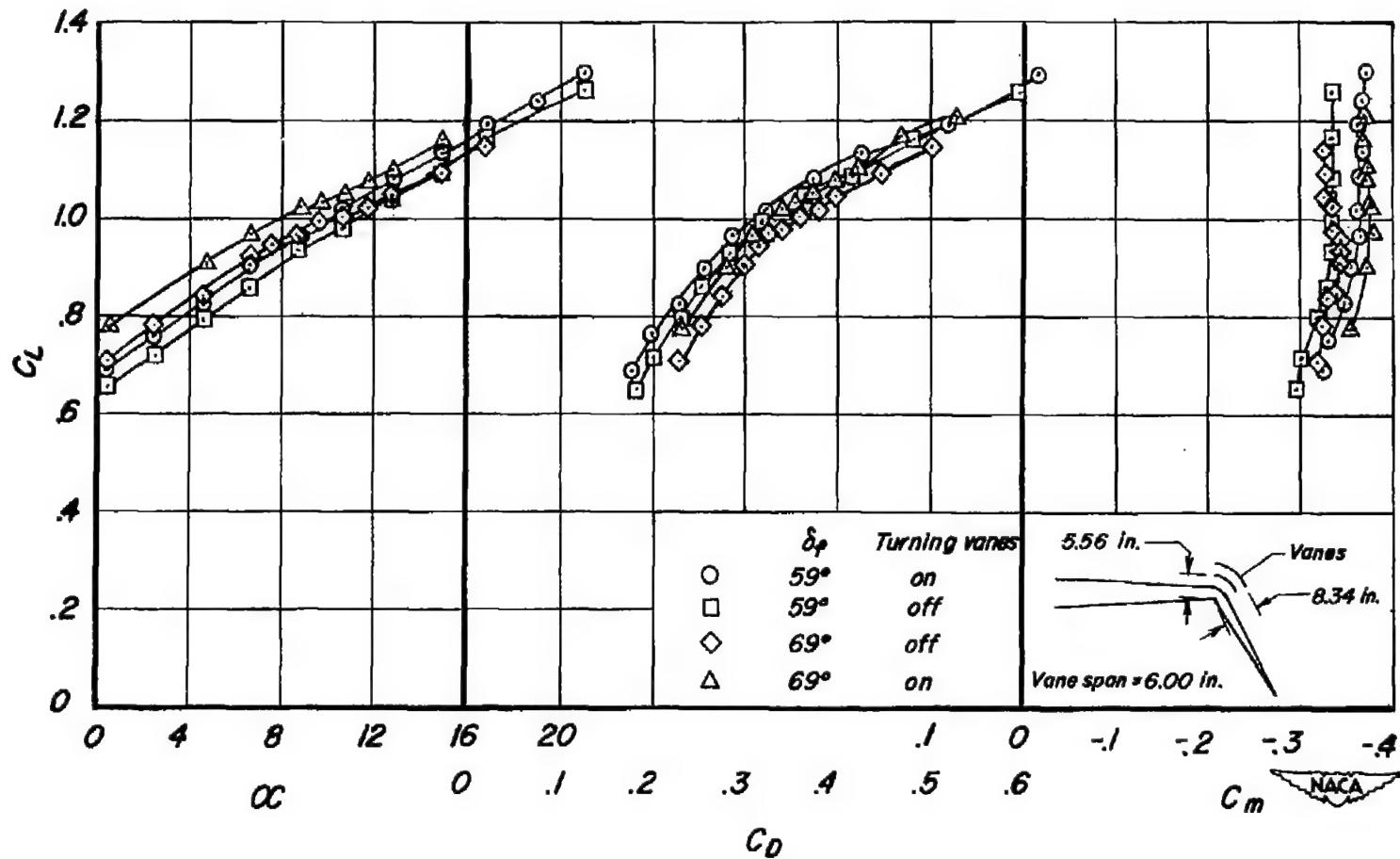


Figure 18.- Aerodynamic characteristics of the model with the flap deflected and with turning vanes at the flap root; suction on.

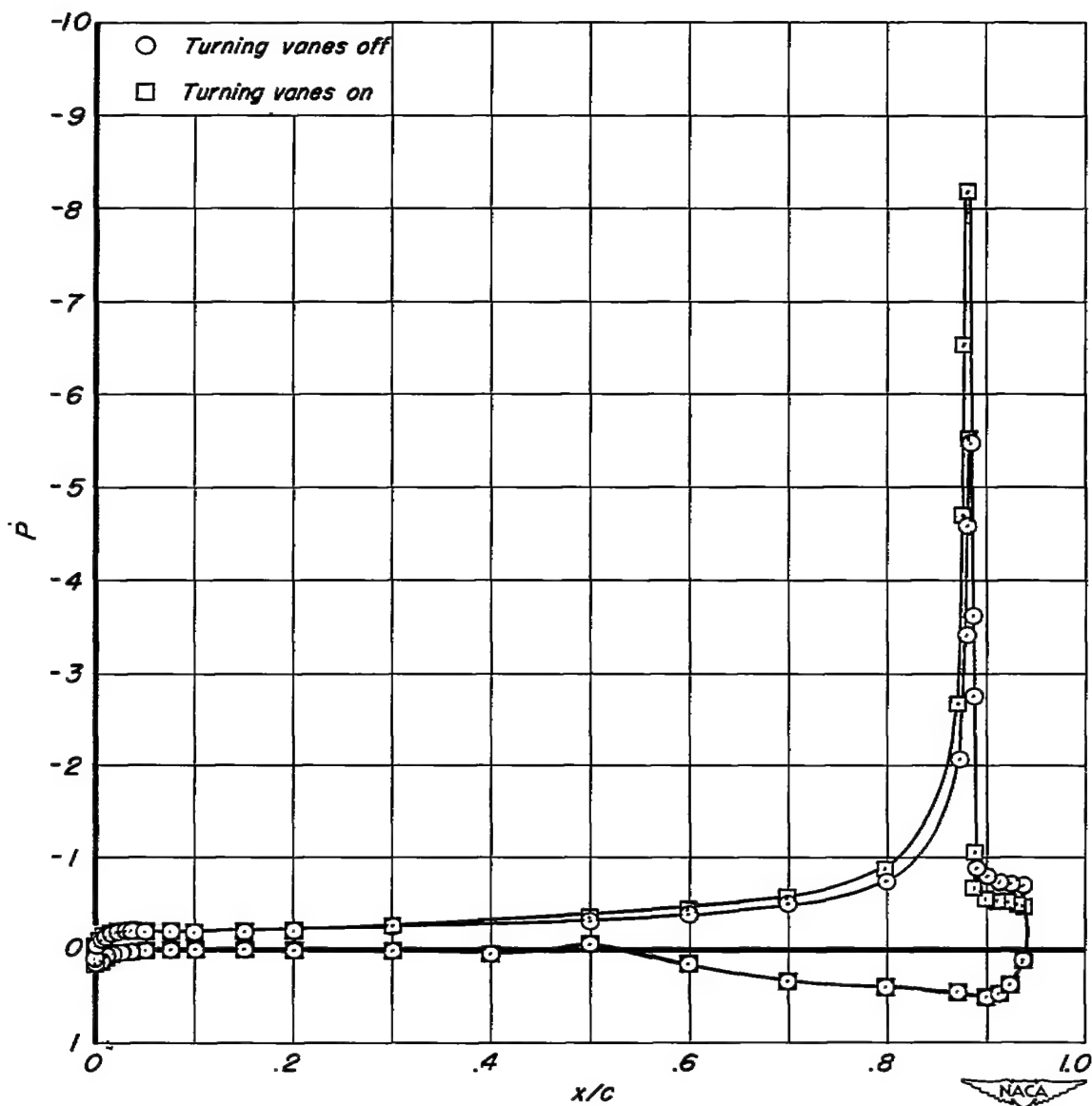


Figure 19.- Chordwise pressure distribution at $\eta = 0.25$ for the model with and without turning vanes at the flap root; $\delta_f = 59^\circ$, $\alpha = 0.5^\circ$, suction on.

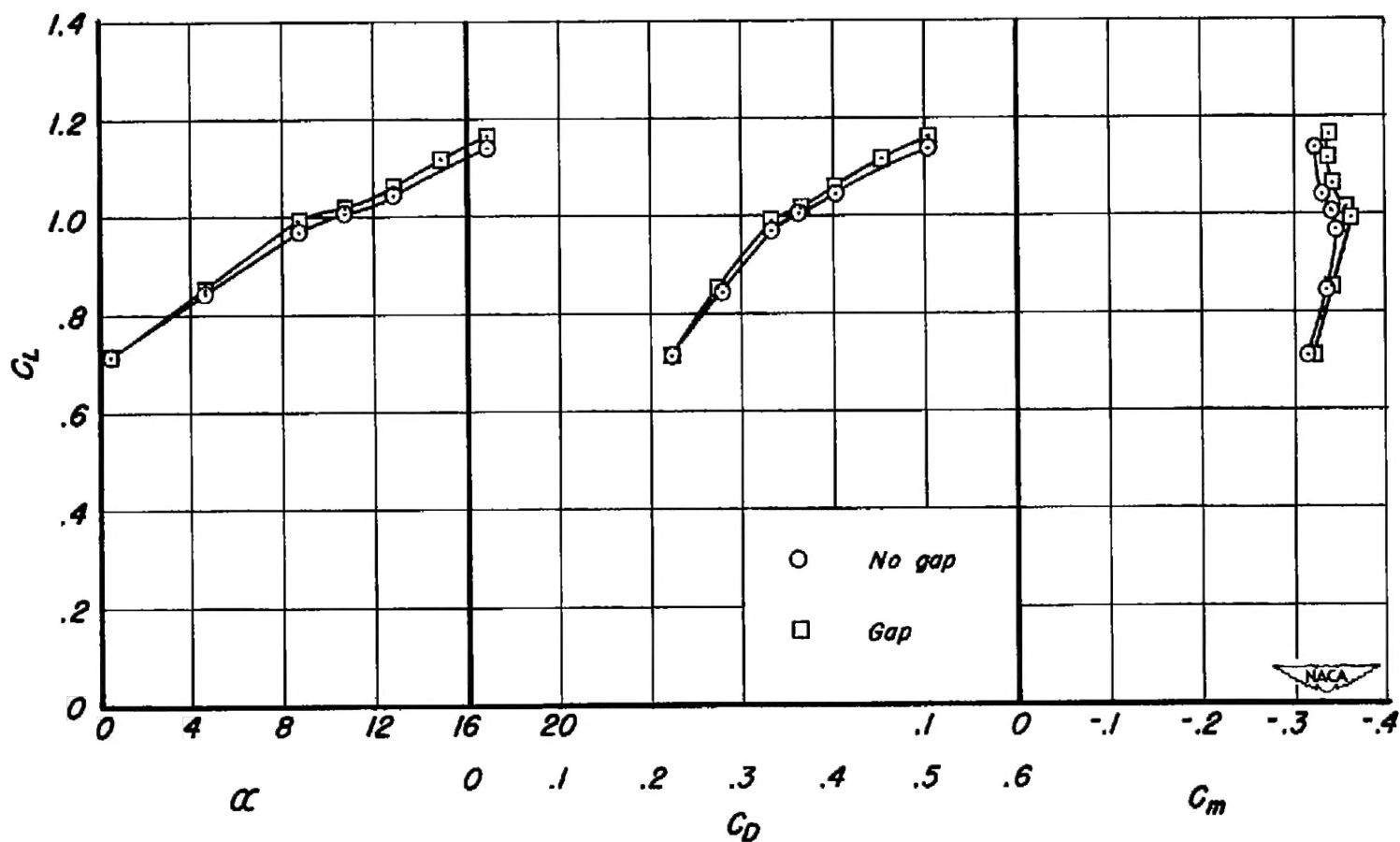


Figure 20.- Aerodynamic characteristics of the model with a gap cut between the fuselage and the flap root; suction on, $\delta_f = 69^\circ$, $\alpha = 0.5^\circ$.

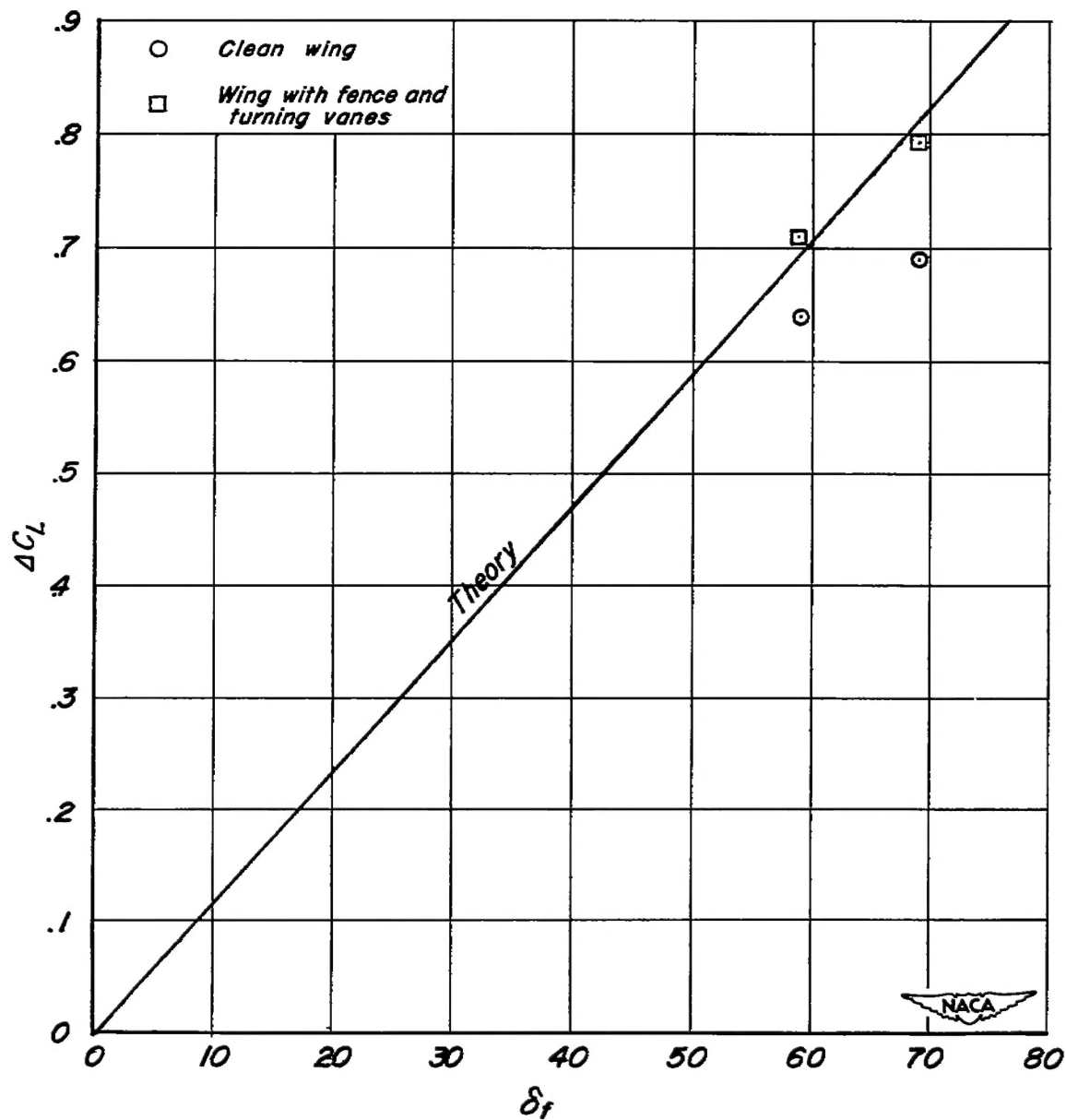


Figure 21.- Comparison of experimental flap lift increment with theory;
 $\alpha = 0^\circ$.

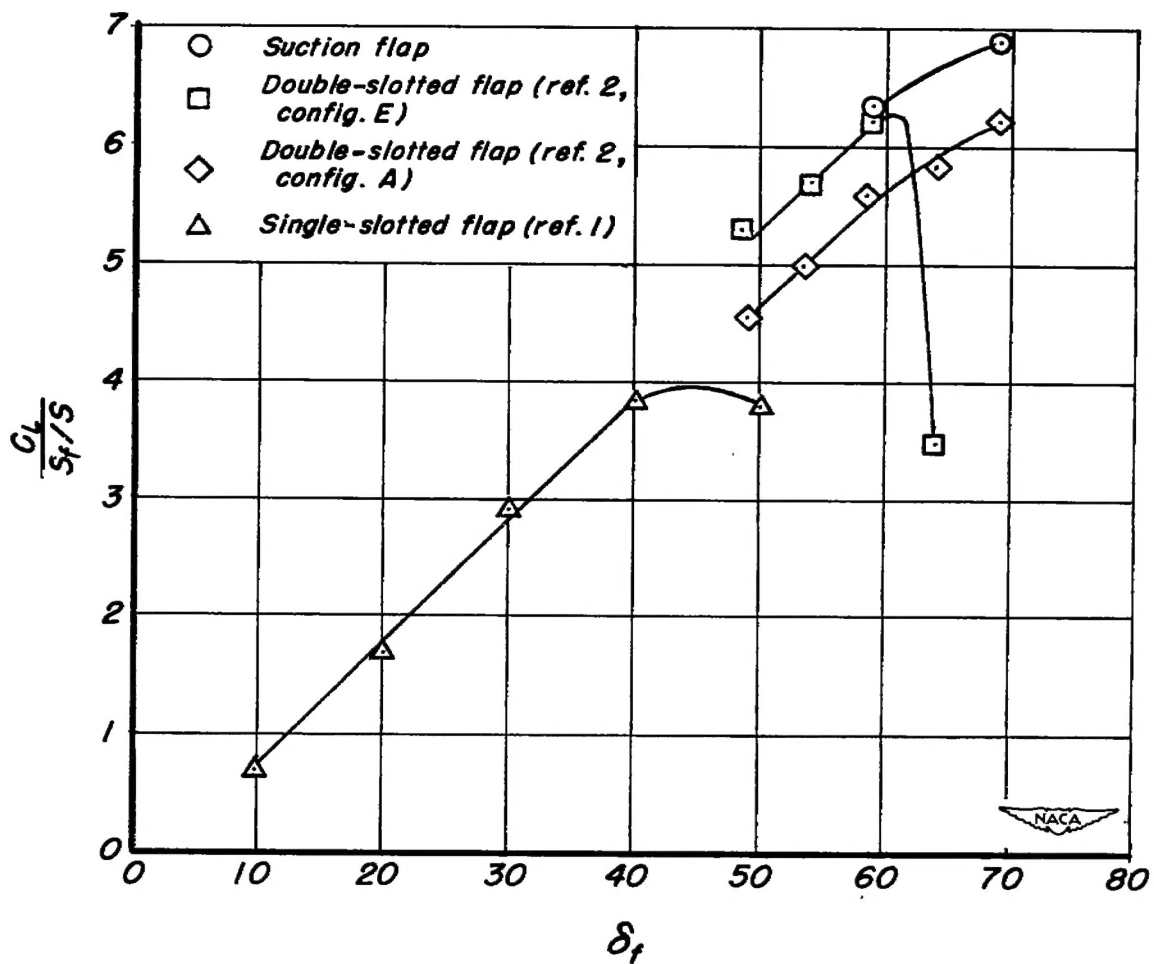


Figure 22.- Comparison of suction flap with single- and double-slotted flaps; $\alpha = 0^\circ$.

~~CONFIDENTIAL~~

